

1 **α -Synuclein strains that cause distinct pathologies differentially inhibit proteasome**

2

3 Genjiro Suzuki^{1*}, Sei Imura^{1,2}, Masato Hosokawa¹, Ryu Katsumata¹, Takashi Nonaka¹, Shin-Ichi
4 Hisanaga², Yasushi Saeki³ and Masato Hasegawa^{1*}

5

6 ¹Department of Dementia and Higher Brain Function, Tokyo Metropolitan Institute of Medical
7 Science, Tokyo, Japan. ²Laboratory of Molecular Neuroscience, Department of Biological
8 Sciences, Tokyo Metropolitan University, Tokyo, Japan. ³Laboratory of Protein Metabolism,
9 Tokyo Metropolitan Institute of Medical Science, Tokyo, Japan.

10

11 E-mail: suzuki-gj@igakuken.or.jp, hasegawa-ms@igakuken.or.jp

12 TEL: +81-3-6834-2349

13

14

1 **Abstract**

2

3 Abnormal α -synuclein aggregation has been implicated in several diseases and is known to
4 spread in a prion-like manner. There is a relationship between protein aggregate structure
5 (strain) and clinical phenotype in prion diseases, however, whether differences in the strains of
6 α -synuclein aggregates account for the different pathologies remained unclear. Here, we generated
7 two types of α -synuclein fibrils from identical monomer and investigated their seeding and
8 propagation ability in mice and primary-cultured neurons. One α -synuclein fibril induced
9 marked accumulation of phosphorylated α -synuclein and ubiquitinated protein aggregates, while
10 the other did not, indicating the formation of α -synuclein two strains. Notably, the former
11 α -synuclein strain inhibited proteasome activity and co-precipitated with 26S proteasome
12 complex. Further examination indicated that structural differences in the C-terminal region of
13 α -synuclein strains lead to different effects on proteasome activity. These results provide a
14 possible molecular mechanism to account for the different pathologies induced by different
15 α -synuclein strains.

16

17

18

1 **Introduction**

2 Misfolding and aggregation of normally soluble proteins are common pathological features of
3 many neurodegenerative diseases, including Alzheimer's, Parkinson's, Creutzfeldt–Jacob and
4 Huntington's diseases (Ross & Poirier, 2004). For example, Parkinson's disease (PD), dementia
5 with Lewy bodies (DLB) and multiple system atrophy (MSA) are characterized by
6 accumulation of misfolded α -synuclein in neuronal and/or glial cells, and therefore these
7 diseases are termed α -synucleinopathies. In PD and DLB, α -synuclein pathologies are mainly
8 observed in neurons in the form of Lewy bodies (LBs) and Lewy neurites (LNs) (Baba et al.,
9 1998), while glial cytoplasmic inclusions (GCIs) are seen in oligodendrocytes in MSA
10 (Wakabayashi, Yoshimoto, Tsuji, & Takahashi, 1998). The abnormal α -synuclein observed in
11 brains of patients is accumulated as fibrous or filamentous forms with cross- β structures (Araki
12 et al., 2019; Spillantini et al., 1997), existing in phosphorylated and partially ubiquitinated states
13 (Fujiwara et al., 2002; Hasegawa et al., 2002). These abnormal α -synuclein species exhibit
14 seeding activity for prion-like conversion, being similar in this respect to the infectious forms of
15 prion protein (PrP) causing Creutzfeldt-Jakob disease (CJD) and bovine spongiform
16 encephalopathy (Goedert, 2015). Various other neurodegenerative disease-related proteins,
17 including amyloid- β , tau and TDP-43, can also propagate through neural networks in a similar
18 manner.

19 α -Synuclein is a natively unfolded protein of 140 amino acid residues, normally found in both
20 soluble and membrane-associated fractions and localized in synaptic termini. Although its
21 physiological function has not been fully clarified, it appears to be involved in the regulation of
22 SNARE complex and in dopamine production. Disease-linked missense mutations and
23 multiplication of the *SNCA* gene encoding α -synuclein have been reported in familial forms of
24 α -synucleinopathies, indicating that structural changes and overexpression of α -synuclein
25 protein are involved in the development of α -synucleinopathies (Wong & Krainc, 2017).

1 Recombinant soluble α -synuclein proteins purified from bacterial cells form amyloid-like fibrils
2 that are morphologically and physicochemically similar to those observed in patients' brains
3 (Araki et al., 2019; Goedert, 2015). These synthetic α -synuclein fibrils can act as seeds and
4 induce seeded aggregation of α -synuclein in cultured cells or primary cultured neurons, as well
5 as in animal brains. Intracerebral inoculation of synthetic α -synuclein fibrils induces
6 phosphorylated and ubiquitinated α -synuclein pathologies even in wild-type (WT) mice (Luk et
7 al., 2012; Masuda-Suzukake et al., 2013). It has also been reported that extracts from brains of
8 patients with α -synucleinopathies induce α -synuclein pathologies in cellular and animal models
9 (Bernis et al., 2015; Watts et al., 2013). In addition, recent studies have suggested that
10 α -synuclein strains with distinct conformations exist, which is a characteristic of prions
11 (Bousset et al., 2013; Gribaudo et al., 2019; Guerrero-Ferreira et al., 2019; Peelaerts &
12 Baekelandt, 2016; Peelaerts et al., 2015; Shahnawaz et al., 2020; Woerman et al., 2019).
13 Synthetic α -synuclein fibrils formed under different physiological conditions *in vitro* show
14 distinct seeding activities and cytotoxicity in cultured cells and rat brains. Furthermore, MSA
15 brain extracts exhibit distinct infectivity compared to PD or control brain extracts in cultured
16 cells or mice expressing mutant A53T or WT α -synuclein (Lau et al., 2019; Peng et al., 2018;
17 Prusiner et al., 2015; Woerman et al., 2019; Woerman et al., 2015).
18 These observations support the idea that α -synuclein shows prion-like behavior, because they
19 can be accounted for by a typical hallmark of the prion phenomenon, i.e., the presence of strains.
20 In prion diseases, the variety of strains that can be differentiated in terms of the clinical signs,
21 incubation period after inoculation, and the vacuolation lesion profiles in the brain of affected
22 animals is due to structural differences of PrP aggregates, as identified by biochemical analyses
23 including glycosylation profile, electrophoretic mobility, protease resistance, and
24 sedimentation. These PrP strains are thought to correspond to different conformations of PrP
25 aggregates, as demonstrated for the yeast prion [*PSI*⁺], which induces aggregates of Sup35p

1 (Ohhashi, Ito, Toyama, Weissman, & Tanaka, 2010). Thus, as the case of prion disease,
2 differences of lesions among α -synucleinopathies might be caused by conformational
3 heterology of α -synuclein assemblies, probably amyloid-like fibrils. However, little is known
4 about how conformational differences of protein aggregates induce a variety of lesions, not only
5 in prion disease, but also in other neurodegenerative diseases, such as α -synucleinopathies.
6 In this study, we prepared two α -synuclein assemblies from identical wild-type α -synuclein
7 monomer under different conditions, and established that they have distinct conformations, i.e.,
8 we succeeded to generating two α -synuclein fibrils from the same monomer. We examined their
9 seeding abilities to convert endogenous soluble α -synuclein monomers into phosphorylated
10 aggregates in mice and primary-cultured neurons, indicating the formation of two α -synuclein
11 strains. Notably, only one strain induced the accumulation of ubiquitinated proteins, as well as
12 phosphorylated α -synuclein aggregates, indicating the ability of this strain to inhibit proteasome
13 activity. Moreover, only this strain strongly inhibited proteasome activity and co-precipitated
14 with purified 26S proteasome complex *in vitro*. Structural studies suggested that the C-terminal
15 region plays a key role in the different properties of the two strains. Taken together, these results
16 provide a possible molecular mechanism to account for the different lesions induced by distinct
17 α -synuclein strains.

18

19

20 **Results**

21 **Formation of Amyloid-like Fibrils from α -Synuclein Proteins *in vitro***

22 We generated two distinct α -synuclein assemblies from the identical purified α -synuclein
23 monomer using the method described in the previous report, with minor modifications (*Figure*
24 *1A*)(Bousset et al., 2013; Lau et al., 2019). Specifically, we prepared recombinant α -synuclein
25 monomer and agitated it in the presence or absence of salt at a physiological concentration. In

1 the presence of physiological salt (30 mM Tris, pH 7.5, 150 mM KCl), the monomer formed a
2 cloudy solution of assemblies with higher turbidity, while in the absence of salt (30 mM Tris,
3 pH 7.5), a clear solution containing assemblies with lower turbidity was formed (*Figure 1A and*
4 *B*). Almost all of the α -synuclein was present as aggregates rather than soluble oligomers under
5 both conditions (*Figure 1-figure supplement 1*)(Thibaudeau, Anderson, & Smith, 2018). Both
6 assemblies showed fibrillar morphology, but the previously reported ribbon-like morphology
7 was not observed (*Figure 1C*)(Bousset et al., 2013). Therefore, we will refer to the former
8 assemblies as α -synuclein fibrils (+) and the later assemblies as α -synuclein fibrils (-). Both
9 fibrils were stained with Thioflavin T and Congo red, indicating their amyloid-like nature.
10 However, the slightly higher Thioflavin T fluorescence and Congo red binding of α -synuclein
11 fibrils (+) suggested that these fibrils have a slightly higher beta-sheet content than α -synuclein
12 fibrils (-) (*Figure 1D and 1E*). Next, we examined the *in vitro* seeding activity of these fibrils.
13 As expected, α -synuclein fibrils (+) showed higher seeding activity than α -synuclein fibrils (-)
14 *in vitro* (*Figure 1F*). These results indicated that we had successfully prepared two distinct types
15 of α -synuclein fibrils from the same monomer.

16

17 **Formation of Phospho- α -Synuclein Pathology by Injection of α -Synuclein Strains into** 18 **Mouse Brain**

19 We next investigated whether there was a strain-dependent difference of prion-like
20 propagation in mouse brain. We injected α -synuclein fibrils (+) and α -synuclein fibrils (-) into
21 striatum of wild-type mice, and after one month, we examined the accumulation of
22 phosphorylated α -synuclein deposits resembling those observed in patients' brains (Luk et al.,
23 2012; Masuda-Suzukake et al., 2013). In contrast to the *in vitro* seeding activities, α -synuclein
24 fibrils (-) induced Lewy body/Lewy neurite-like abnormal phosphorylated α -synuclein deposits
25 through the mouse brain, including striatum, corpus callosum and cortex (*Figure 2A and Figure*

1 2-figure supplement 1), whereas few phosphorylated α -synuclein deposits were induced by
2 α -synuclein fibrils (+) (Figure 2B and Figure 2-figure supplement 1). The deposits induced by
3 α -synuclein fibrils (-) were also positive for ubiquitin staining, like Lewy bodies and Lewy
4 neurites (Figure 2C and D). Thus, there was a strain-dependent difference of α -synuclein fibril
5 formation from the identical α -synuclein monomer when the two strains were inoculated into
6 the mouse brain, and α -synuclein fibrils (-) had higher prion-like seeding activity than
7 α -synuclein fibrils (+) in mouse brain, contrary to the in vitro seeding results (Figure 1F).

8

9 **Formation of Phospho- α -Synuclein Pathology Induced by the Two α -Synuclein Strains in** 10 **Cultured Neurons**

11 To further study the difference in the formation of pathological α -synuclein aggregates in
12 neurons, we compared the ability of the two α -synuclein strains to induce seed-dependent
13 aggregation of α -synuclein in primary-cultured neurons. When primary-cultured neurons from
14 non-transgenic mice were treated with α -synuclein fibrils for two weeks, we observed a
15 dramatic increase of phosphorylated α -synuclein accumulation only in the case of α -synuclein
16 fibrils (-), while little accumulation was seen with α -synuclein fibrils (+) (Figure 3A and B).
17 These results are consistent with those observed in the mouse brain.

18 Next, we performed biochemical analysis of detergent-insoluble α -synuclein prepared from
19 these cells. Phosphorylated α -synuclein were accumulated in cells treated with both α -synuclein
20 fibrils (-) and α -synuclein fibrils (+) (Figure 3C). However, α -synuclein fibrils (-) induced a
21 greater accumulation of phosphorylated α -synuclein than did α -synuclein fibrils (+) (Figure 3C).
22 The phosphorylated and aggregated α -synuclein in these cells was found to be endogenous
23 mouse α -synuclein, indicating that the introduced human α -synuclein fibrils worked as seeds
24 (Figure 3D). We also examined the accumulation of detergent-insoluble ubiquitinated proteins
25 by immunofluorescence and immunoblot analyses and found that not only ubiquitinated

1 α -synuclein, but also other ubiquitinated proteins were accumulated in cells treated with
2 α -synuclein fibrils (-). There was no significant increase of ubiquitinated protein accumulation
3 in cells treated with α -synuclein fibrils (+) (*Figure 3A and E*). These results indicated that only
4 α -synuclein fibrils (-) induced much accumulation of phosphorylated α -synuclein and
5 ubiquitinated proteins in primary-cultured neurons, in accordance with the findings in mouse
6 brain.

7

8 **Different Interactions of α -Synuclein Strains with 26S Proteasome**

9 The above results motivated us to examine proteasome activity in the presence of these two
10 types of α -synuclein fibrils. We purified 26S proteasome complex from budding yeast
11 expressing FLAG-tagged Rpn11p, a subunit of 19S regulatory complex (*Figure 4-figure*
12 *supplement 1*)(Saeki, Isono, & Toh, 2005). The activity of the purified 26S proteasome was
13 examined in the presence or absence of α -synuclein fibrils. The eukaryotic proteasome has three
14 active subunits, β 1, β 2 and β 5, each displaying a specific catalytic activity, trypsin-like,
15 chymotrypsin-like and caspase-like activity, respectively. Thus, we examined the
16 chymotrypsin-like (*Figure 4A*), caspase-like (*Figure 4B*) and trypsin-like (*Figure 4C*) activities
17 of 26S proteasome in the presence of these α -synuclein fibrils using each fluorogenic peptide
18 substrate in vitro. The catalytic activity of 26S proteasome was drastically impaired in the
19 presence of α -synuclein fibrils (-), whereas α -synuclein fibrils (+) were ineffective (*Figure*
20 *4A-C*). These results accord with our mouse and primary-cultured neuron data, i.e., only
21 α -synuclein fibrils (-) could induce much accumulation of phosphorylated α -synuclein and
22 ubiquitinated proteins. Co-aggregation of functional proteins with misfolded protein aggregates
23 may cause the impairment of their function. Therefore, we investigated the interaction of 26S
24 proteasome with the fibrils. α -Synuclein fibrils were mixed with purified 26S proteasome, and
25 the mixture was centrifuged. The supernatant and pellet fractions were analyzed by western

1 blotting. We found that both α -synuclein fibrils (-) and α -synuclein fibrils (+) were fractionated
2 to the pellet fractions (*Figure 4D*). However, only α -synuclein fibrils (-) co-precipitated with
3 26S proteasome, while α -synuclein fibrils (+) did not (*Figure 4E*). Taken together, these results
4 indicate that only α -synuclein fibrils (-) interact with 26S proteasome and impair the proteasome
5 activity.

6 If α -synuclein fibrils (-) bind other proteins, such as 26S proteasome, while α -synuclein fibrils
7 (+) do not, the structures of the two types of fibrils should be distinguishable. Indeed, we did
8 observe slight differences between these two types of fibrils (*Figure 1*). Amyloid-like fibrils are
9 composed of core regions consisting of β -sheet-rich rigid structure, and exposed regions, which
10 might interact with other molecules. The core regions tend to be resistant to protease attack,
11 whereas exposed regions tend to be easily digested by protease. To identify the core regions and
12 exposed regions of these α -synuclein fibrils, we carried out limited proteolysis with proteinase
13 K, followed by mass spectrometric analysis (*Figure 4F*) (Suzuki, Shimazu, & Tanaka, 2012).
14 We found that α -synuclein fibrils (-) have a smaller core region (amino acid residues 39-96 and
15 40-94; m/z 5656 and 5268, respectively) corresponding to the NAC region (amino acid residues
16 61-95), which had previously been reported as the core region of α -synuclein fibrils
17 (Guerrero-Ferreira et al., 2018; Li et al., 2018). In contrast, α -synuclein fibrils (+) had a larger
18 core region, extending to the C-terminal regions (residues 31-109, 28-118 and 25-132; m/z 7860,
19 9115 and 10907, respectively), indicating that α -synuclein fibrils (-) have amyloid structure with
20 a more exposed C-terminal region than α -synuclein fibrils (+). To confirm these results, we
21 performed dot-blot analysis using various antibodies against different regions of α -synuclein
22 protein. Native α -synuclein fibrils were spotted on nitrocellulose membranes and detected by
23 applying various α -synuclein antibodies. Antibodies raised against the N-terminal region of
24 α -synuclein (residues 1-10) and the NAC region (91-99) almost equally recognized both types
25 of α -synuclein fibrils, indicating that they have similar structure in the N-terminal and NAC

1 regions (*Figure 4G*). However, as expected from the above data, the antibodies raised against
2 C-terminal regions (amino acid 115-122 and 131-140) bound more strongly to α -synuclein
3 fibrils (-) than to α -synuclein fibrils (+), supporting the idea that the C-terminal region of
4 α -synuclein fibrils (-) is more exposed than that of α -synuclein fibrils (+). Thus, we considered
5 that the C-terminal region of α -synuclein fibrils (-) might interact with 26S proteasome and
6 impair its activities. Indeed, we previously reported that C-terminally truncated α -synuclein
7 fibrils induced pathology in mouse brain less potently than did full-length α -synuclein fibrils,
8 even though the C-terminally truncated α -synuclein fibrils had higher seeding activity in vitro
9 (Terada et al., 2018). To confirm this, we next examined the seeding activity of C-terminally
10 truncated fibrils formed in the absence of salt in primary-cultured neurons. We prepared
11 C-terminally truncated α -synuclein monomer (residues 1-120) and agitated it in the absence of
12 salt. The resulting assemblies showed fibrillar morphology and thioflavin T binding (data not
13 shown), and we refer to them as Δ C20 fibrils (-). We treated mouse primary-cultured neurons
14 with Δ C20 fibrils (-) and examined the accumulation of phosphorylated α -synuclein and
15 ubiquitinated proteins. As expected, we observed little accumulation (*Figure 4-figure*
16 *supplement 2*). Considering all these results, we can conclude that the C-terminal region of
17 α -synuclein is exposed only in α -synuclein fibrils (-) and this region interacts with 26S
18 proteasome and impairs its activity.

19

20

21 **Discussion**

22 According to the prion hypothesis, differences in disease symptoms and lesions are caused by
23 differences in the conformation of strains. Therefore, if α -synuclein is prion-like, differences in
24 the structure of α -synuclein aggregates should cause the differences in the lesions observed in
25 various α -synucleopathies. Recent analyses have shown that introduction of extracts from brains

1 of patients with PD and MSA into mice and cells induces different pathologies (Prusiner et al.,
2 2015; Tarutani, Arai, Murayama, Hisanaga, & Hasegawa, 2018; Woerman et al., 2019;
3 Woerman et al., 2015). Similar results were obtained with brain extracts of patients with
4 tauopathies, in which tau is abnormally accumulated (Narasimhan et al., 2017; Saito et al.,
5 2019). Moreover, it has been clarified that TDP-43 aggregates have a different structure
6 depending on the disease, and different lesions appear when the patients' brain extracts are
7 introduced into cells or animals (Laferrriere et al., 2019; Nonaka et al., 2013; Porta et al., 2018;
8 Tsuji et al., 2012). As for α -synuclein, it has been reported that aggregates having different
9 structures are formed *in vitro* (Bousset et al., 2013; Shahnawaz et al., 2020), and the lesions
10 caused by introduction of aggregates having different structures into cells and rodents are
11 different (Gribaudo et al., 2019; Lau et al., 2019; Peelaerts et al., 2015). However, it has
12 remained unclear what molecular mechanism might lead to the differences in phenotypes
13 induced by different protein aggregates.

14 In this study, we confirmed that different pathologies were caused by two α -synuclein strains
15 with different structures, and we also found that these α -synuclein strains differ in their ability
16 to inhibit 26S proteasome activity. It has already been reported that protein aggregates that can
17 cause neurodegenerative diseases may interact with proteasome and inhibit its activity (Bence,
18 Sampat, & Kopito, 2001; Thibaudeau et al., 2018; Zondler et al., 2017). However, it is a
19 noteworthy finding in this work that one of the two differently structured fibrils formed from
20 identical monomer under different conditions inhibited proteasome, while the other did not.
21 This clearly raises the possibility that inhibition of proteasome by abnormal α -synuclein plays a
22 role in the pathology. These results provide a possible molecular mechanism to account for the
23 different lesions induced by distinct α -synuclein strains. Considering that PD and MSA have
24 different structures of accumulated α -synuclein (Klingstedt et al., 2019; Lau et al., 2019;
25 Prusiner et al., 2015; Shahnawaz et al., 2020; Woerman et al., 2019; Woerman et al., 2015), it

1 seems highly likely that the structures of α -synuclein fibrils determine the lesions observed in
2 these diseases.

3 Protein inclusions found in many neurodegenerative diseases are often ubiquitinated, and this is
4 consistent with reports that ubiquitin proteasome systems are impaired in neurons of patients
5 with neurodegenerative diseases (Bence et al., 2001). Recently, it was reported that protein
6 aggregates co-aggregate with proteasome at the molecular level (Guo et al., 2018). Furthermore,
7 α -synuclein oligomers, A β oligomers and polyglutamine inhibit 20S proteasome (Thibaudeau et
8 al., 2018). In our α -synuclein fibril formation experiments, almost all the proteins formed
9 insoluble aggregates, and soluble oligomers could not be isolated (*Figure 1-figure supplement*
10 *1*). Thus, our results indicate that protein aggregates may also show proteasome-inhibitory
11 activity, and the extent of the inhibitory activity depends on the structure of the aggregates.
12 These facts indicate that pathogenic protein oligomers and aggregates have different effects on
13 cells depending on their structure, and both may be toxic.

14 Our results suggest that the difference in the structure of the two strains is mainly at the
15 C-terminal region. The C-terminal region (residues 96-140) of α -synuclein is acidic and
16 contains negatively charged residues, including aspartate and glutamate, as well as proline
17 residues. When intermolecular repulsion at the C-terminal region is weakened by changes in
18 ionic strength, exposure of the C-terminal region decreases, and more tightly packed
19 α -synuclein fibrils are formed in the presence of salt. On the other hand, in the absence of salt,
20 intermolecular repulsion at the C-terminal region causes the formation of α -synuclein fibrils in
21 which the C-terminal region is exposed. Only this latter type of α -synuclein fibrils can interact
22 with 26S proteasome complex in vitro, causing inhibition of 26S proteasome activity. If this
23 also occurs in cells, abnormal α -synuclein aggregates, which might be partially degraded by
24 proteasome, would be accumulated (*Figure 4-figure supplement 3*). Consequently,
25 phosphorylated and ubiquitinated α -synuclein aggregates would be accumulated in neurons and

1 then presumably would propagate throughout the brain in a prion-like manner. Our results
2 imply that inhibition of proteasome activity by protein aggregates is critical for prion-like
3 propagation of these protein aggregates. Thus, inhibiting the interaction between aggregates and
4 the proteasome may be a promising therapeutic strategy for neurodegenerative diseases.
5 Forming fibrils from purified monomeric protein and introducing them into cells or animals
6 might be a useful approach for analyzing the mechanisms of propagation and toxicity of
7 diseases in which protein aggregates accumulate. However, based on our results and previous
8 reports, it seems possible that the results obtained might vary markedly in response to even
9 slight differences in the structure of the introduced fibrils (Bousset et al., 2013; Gribaudo et al.,
10 2019; Peelaerts et al., 2015). Introducing brain extract from a patient with a neurodegenerative
11 disease into cells or animals would also be one approach for identifying the cause of the disease
12 and developing a treatment, but even in patients with the same disease, the results might vary
13 due to slight differences in the structure of the accumulated protein aggregates. Therefore, when
14 conducting such experiments, it is extremely important to analyze the structure of the protein
15 aggregates.
16 In this study, we found that the degree of interaction with proteasome and the inhibition of
17 proteasome activity vary depending on the strain of α -synuclein aggregates. The relationship
18 between proteasome inhibition and the induction of the pathology supports the hypothesis that
19 prion-like activity of α -synuclein aggregates contributes to disease progression.

20

21

22 **Materials and methods**

23 **Antibodies**

24 Anti-phosphorylated α -synuclein antibodies to pSer129 including #64 (Fujiwara et al., 2002)
25 and EP1536Y (Abcam), and other anti- α -synuclein antibodies including 1-10 (Cosmo Bio),

1 NAC1 (a gift from Dr. Jäkälä), 131-140 (Cosmo Bio), LB509 (Santa Cruz Biotechnology),
2 D37A6 (Cell Signaling Technology) were used. Anti-ubiquitin antibody (Proteintech),
3 anti-GAPDH antibody (Millipore) and anti-FLAG antibody (Sigma) were also used.
4 HRP-labeled antibodies (Invitrogen), Alexa Fluor 488 and Alexa Fluor 568 conjugated
5 antibodies (Thermo Fisher Scientific) were used as secondary antibodies.

6 **Expression and purification of Recombinant Wild-type and C-Terminally Truncated**

7 **Human α -Synuclein**

8 Full-length and C-terminally truncated α -synuclein encoded in pRK172 plasmids were
9 transformed into *Escherichia coli* BL21 (DE3). Recombinant proteins were purified as
10 described previously (Nonaka, Watanabe, Iwatsubo, & Hasegawa, 2010). Protein concentration
11 was determined by HPLC.

12 **Preparation of α -Synuclein Fibrils**

13 α -Synuclein fibrils were prepared as follows. Purified recombinant α -synuclein proteins were
14 dissolved in 30 mM Tris-HCl, pH 7.5, containing 150 mM KCl and 0.1% NaN₃, to a final
15 concentration of 6 mg/ml. The samples were incubated at 37 °C under rotation at 20 rpm for 7
16 days. The assembled α -synuclein was sonicated with an ultrasonic homogenizer (VP-5S,
17 TAITEC) in 30 mM Tris-HCl, pH 7.5. For the measurement of turbidity, the resultant
18 α -synuclein assemblies were diluted to 1 mg/ml and the absorbance at 440 nm was measured.

19 **Transmission Electron Microscopy**

20 α -Synuclein fibrils were diluted to 15 μ M in 30 mM Tris-HCl, pH 7.5, plated on carbon-coated
21 300-mesh copper grids (Nissin EM), and stained with 2% [v/v] phosphotungstate. Micrographs
22 were recorded on a JEM-1400 electron microscope (JEOL).

23 **Thioflavin T-binding Assay**

24 The degree of fibrillation was measured in terms of Thioflavin T (ThT) fluorescence intensity,
25 which increases when ThT binds to amyloid-like fibrils. The samples (7.5 μ M) were incubated

1 with 20 μ M ThT in 30 mM Tris-HCl buffer (pH 7.5) for 30 min at 37 °C. Fluorometry was
2 performed using a microplate reader (Infinite 200, TECAN, excitation 442 nm, emission 485
3 nm).

4 **Congo Red Binding Assay**

5 The binding of Congo red was measured as described previously (Suzuki et al., 2012). α -Syn
6 monomer and fibrils (37.5 μ M) were mixed with Congo red (1 μ M) and incubated for 1 hour at
7 37 °C. Absorbance between 400 and 700 nm was measured with a plate reader (Infinite 200,
8 TECAN). The binding of Congo red was calculated as $A_{540}/25296 - A_{477}/46306$.

9 **α -Synuclein Aggregation Assay**

10 Full-length α -synuclein aggregation experiments were performed using a microplate reader
11 (Infinite 200, TECAN, excitation 442 nm, emission 485 nm) and monitored by measuring ThT
12 fluorescence in the absence or presence of 5% α -syn fibril seeds. All experiments were
13 performed at 37 °C, under quiescent conditions in flat-bottomed 96-well black plates
14 (Sumitomo Bakelite) sealed with MicroAmp Optical Adhesive Film (Applied Biosystems). The
15 reaction mixture consisted of PBS containing 1 mg/ml α -synuclein monomer. During
16 experiments under quiescent conditions, ThT fluorescence was read every 2 min.

17 **Primary-cultured neurons and Introduction of α -Synuclein Proteins into Cells**

18 Dissociated cultures of embryonic (E15) mouse neurons were prepared from pregnant C57BL/6
19 mice using Neuron Dissociation Solutions (FUJI FILM Wako) according to the manufacturer's
20 protocol. Briefly, dissected brain was digested with enzyme solution for 30 min at 37 °C, then
21 centrifuged. Dispersion solution was added and tissues were suspended, then isolation solution
22 was added. Cells were collected by centrifugation, resuspended and plated on
23 poly-L-lysine-coated cover glass or plates. Neurons were maintained at 37 °C in 5% CO₂ in
24 Neurobasal Medium (Gibco) supplemented with 1x B27 and 1x Glutamax. Neurons were
25 cultured for 7 days in vitro (DIV) in 6-well plates, and then treated with sonicated α -synuclein

1 fibrils diluted in culture medium. Neurons were collected or fixed at 14 days post treatment (21
2 DIV).

3 **Purification of 26S Proteasome from Budding Yeast**

4 Yeast 26S proteasome was purified as described previously (Saeki et al., 2005). Briefly, the
5 yeast strain (BY4741, *Rpn11-FLAGx3::KanMX*) was cultured in YPD for 2 days, harvested,
6 washed and stocked at -80°C. Buffer A'' (50 mM Tris-HCl, pH 7.5, 100 mM NaCl, 10%
7 glycerol, 4 mM ATP, 10 mM MgCl₂) and glass beads were added and the cells were lysed in a
8 Beads Shocker (Yasui Kikai). Cell debris was removed by centrifugation and then anti-FLAG
9 M2 antibody-conjugated agarose beads (Sigma) were added. The mixture was incubated for 2
10 hours at 4°C. Agarose beads were washed with Buffer A'' and Buffer A'' containing 0.1% Triton,
11 and proteasome was eluted by adding 3x FLAG peptide (400 µg/ml) (Sigma) in Buffer A''.

12 **26S Proteasome Activity Assays**

13 Inhibition of α -synuclein fibrils on proteasome activity was measured using fluorogenic
14 peptides in 96-well black flat-bottomed plates. 26S proteasome (10 µg/ml) was added to
15 α -synuclein fibrils (35 µM, calculated based on the monomer protein concentration), and the
16 mixture was incubated in buffer A'' containing 100 µM fluorogenic substrate (suc-LLVY-mca,
17 Z-LLE-mca, Peptide Institute) or 50 µM fluorogenic substrate (boc-LRR-mca, Peptide Institute)
18 for 60 minutes at 37°C. Fluorescence was measured before and after incubation (Infinite 200,
19 TECAN, excitation 360 nm, emission 440 nm). The rate of increase in fluorescence intensity is
20 regarded as representing proteasome activity.

21 **Binding Assay of Proteasome with α -Synuclein Fibrils**

22 α -Synuclein fibrils were mixed with purified 26S proteasome in Buffer A'', and the mixture was
23 centrifuged at 21,500 x g for 20 minutes. The supernatant and pellet fractions were analyzed by
24 the western blotting.

25 **Immunocytochemistry**

1 Introduction of α -synuclein fibrils were conducted as described above, using mouse primary
2 cultured cells grown on coverslips. At 2 weeks after introduction of fibrils, the cells were fixed
3 with 4% paraformaldehyde and treated with the indicated primary antibodies at 1:1000 dilution.
4 After incubation overnight, the cells were washed and treated with secondary antibodies
5 conjugated with Alexa Fluor (Thermo Fisher) for 1 hour. The cells were mounted with DAPI to
6 counterstain nuclear DNA and analyzed with a BZ-X710 (Keyence) and BZ-X analyzer
7 (Keyence).

8 **α -Synuclein Inoculation into Mice and Immunohistochemistry of Mouse Brains**

9 Ten-week-old, male C57BL/6J mice were purchased from CLEA Japan, Inc. All experimental
10 protocols were performed according to the recommendations of the Animal Care and Use
11 Committee of Tokyo Metropolitan Institute of Medical Science. α -Synuclein samples (150 μ M,
12 5 μ l) were injected into the striatum (anterior-posterior, 0.2 mm; medial-lateral, -2.0 mm;
13 dorsal-ventral, 2.6 mm). Inoculation into mouse brain was performed as described previously
14 (Masuda-Suzukake et al., 2013).

15 One month after inoculation, mice were deeply anesthetized with isoflurane (Pfizer) and
16 sacrificed, and the brain was perfused with 0.1 M phosphate buffer. Sections were fixed in 4%
17 paraformaldehyde and preserved in 20% sucrose in 0.01 M phosphate buffered saline, pH 7.4.
18 were cut serially on a freezing microtome at 30 μ m thickness. The sections were then mounted
19 on glass slides. Sections were incubated with 1% H₂O₂ for 30 min to eliminate endogenous
20 peroxidase activity and were treated with 100% formic acid (Wako) for 10 min for antigen
21 retrieval and washed under running tap water. Immunohistochemistry with polyclonal antibody
22 1175 (1:1,000) directed against α -synuclein phosphorylated at Ser129 or anti-ubiquitin (DAKO,
23 1:10,000) were performed as described previously (Masuda-Suzukake et al., 2013). Antibody
24 labeling was performed by incubation with goat anti-rabbit IgG (1:1,000, Vector Laboratories)
25 for 3 hours. The antibody labeling was visualized by incubation with avidin-biotinylated

1 horseradish peroxidase complex (ABC Elite, Vector Laboratories, 1:1,000) for 3 hours, followed
2 by incubation with a solution containing 0.01% 3,3'-diaminobenzidine, 0.05 M imidazole and
3 0.00015% H₂O₂ in 0.05 M Tris-HCl buffer, pH 7.6. Counter nuclear staining was performed
4 with hematoxylin (Muto Pure Chemicals). The sections were then rinsed with distilled water,
5 treated with xylene, and coverslipped with Entellan (Merck). Images were analyzed with a
6 BZ-X710 (Keyence) and BZ-X analyzer (Keyence). We examined three mice for each sample
7 and each mouse yielded highly similar results. Animal experiments were done by the
8 experimenter who is blind.

9 **Sedimentation Analysis and Western blotting**

10 Neurons were harvested, collected by centrifugation (2,000 × g, 5 min) and washed with PBS.
11 The cellular proteins were extracted by sonication in 200 µl of buffer A68 (10 mM Tris-HCl, pH
12 7.5, 1 mM EGTA, 10% sucrose, 0.8 M NaCl) containing sarkosyl (final 1%, w/v) and protease
13 inhibitor (Roche). After ultracentrifugation at 135,000 × g for 20 min at 25 °C, the supernatant
14 was collected as sarkosyl-soluble fraction, and the protein concentration was determined by
15 Bradford assay. The pellet was solubilized in 50 µl of SDS-sample buffer. Both sarkosyl-soluble
16 and insoluble fractions were analyzed by immunoblotting with appropriate antibodies as
17 indicated.

18 **Statistical analysis**

19 Student's *t*-test was performed when comparing 2 groups. One-way ANOVA and Tukey's post
20 hoc test were performed with EZR when comparing 3 groups (Kanda, 2013). P values below
21 0.05 were considered to be statistically significant.

22

23

24 **Acknowledgments**

25 We would like to thank all members of the laboratory for helpful discussion.

1

2

3 **Competing Interests**

4 The authors declare no competing financial interests.

5

6 **References**

- 7 Araki, K., Yagi, N., Aoyama, K., Choong, C. J., Hayakawa, H., Fujimura, H., . . . Mochizuki,
8 H. (2019). Parkinson's disease is a type of amyloidosis featuring accumulation of
9 amyloid fibrils of alpha-synuclein. *Proc Natl Acad Sci U S A*.
10 doi:10.1073/pnas.1906124116
- 11 Baba, M., Nakajo, S., Tu, P. H., Tomita, T., Nakaya, K., Lee, V. M., . . . Iwatsubo, T. (1998).
12 Aggregation of alpha-synuclein in Lewy bodies of sporadic Parkinson's disease and
13 dementia with Lewy bodies. *Am J Pathol*, *152*(4), 879-884.
- 14 Bence, N. F., Sampat, R. M., & Kopito, R. R. (2001). Impairment of the ubiquitin-proteasome
15 system by protein aggregation. *Science*, *292*(5521), 1552-1555.
16 doi:10.1126/science.292.5521.1552
- 17 Bernis, M. E., Babila, J. T., Breid, S., Wusten, K. A., Wullner, U., & Tamguney, G. (2015).
18 Prion-like propagation of human brain-derived alpha-synuclein in transgenic mice
19 expressing human wild-type alpha-synuclein. *Acta Neuropathol Commun*, *3*, 75.
20 doi:10.1186/s40478-015-0254-7
- 21 Bousset, L., Pieri, L., Ruiz-Arlandis, G., Gath, J., Jensen, P. H., Habenstein, B., . . . Melki, R.
22 (2013). Structural and functional characterization of two alpha-synuclein strains.
23 *Nat Commun*, *4*, 2575. doi:10.1038/ncomms3575
- 24 Fujiwara, H., Hasegawa, M., Dohmae, N., Kawashima, A., Masliah, E., Goldberg, M. S., . . .
25 Iwatsubo, T. (2002). alpha-Synuclein is phosphorylated in synucleinopathy lesions.
26 *Nat Cell Biol*, *4*(2), 160-164. doi:10.1038/ncb748
- 27 Goedert, M. (2015). NEURODEGENERATION. Alzheimer's and Parkinson's diseases: The
28 prion concept in relation to assembled Abeta, tau, and alpha-synuclein. *Science*,
29 *349*(6248), 1255-1255. doi:10.1126/science.1255555
- 30 Gribaudo, S., Tixador, P., Bousset, L., Fenyi, A., Lino, P., Melki, R., . . . Perrier, A. L. (2019).
31 Propagation of alpha-Synuclein Strains within Human Reconstructed Neuronal
32 Network. *Stem Cell Reports*, *12*(2), 230-244. doi:10.1016/j.stemcr.2018.12.007
- 33 Guerrero-Ferreira, R., Taylor, N. M., Arteni, A. A., Kumari, P., Mona, D., Ringler, P., . . .
34 Stahlberg, H. (2019). Two new polymorphic structures of human full-length
35 alpha-synuclein fibrils solved by cryo-electron microscopy. *Elife*, *8*.
36 doi:10.7554/eLife.48907

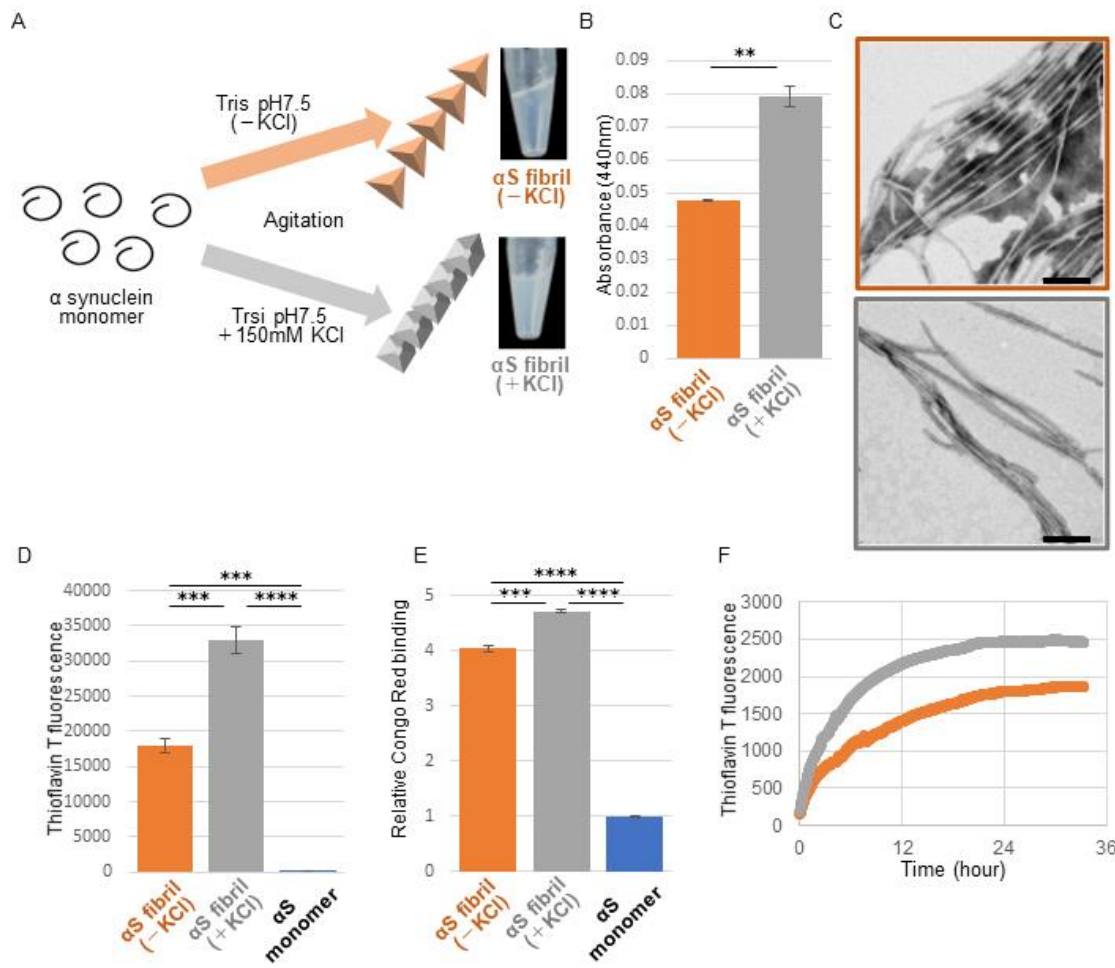
- 1 Guerrero-Ferreira, R., Taylor, N. M., Mona, D., Ringler, P., Lauer, M. E., Riek, R., . . .
2 Stahlberg, H. (2018). Cryo-EM structure of alpha-synuclein fibrils. *Elife*, 7.
3 doi:10.7554/eLife.36402
- 4 Guo, Q., Lehmer, C., Martinez-Sanchez, A., Rudack, T., Beck, F., Hartmann, H., . . .
5 Fernandez-Busnadiego, R. (2018). In Situ Structure of Neuronal C9orf72 Poly-GA
6 Aggregates Reveals Proteasome Recruitment. *Cell*, 172(4), 696-705 e612.
7 doi:10.1016/j.cell.2017.12.030
- 8 Hasegawa, M., Fujiwara, H., Nonaka, T., Wakabayashi, K., Takahashi, H., Lee, V. M., . . .
9 Iwatsubo, T. (2002). Phosphorylated alpha-synuclein is ubiquitinated in
10 alpha-synucleinopathy lesions. *J Biol Chem*, 277(50), 49071-49076.
11 doi:10.1074/jbc.M208046200
- 12 Kanda, Y. (2013). Investigation of the freely available easy-to-use software 'EZR' for medical
13 statistics. *Bone Marrow Transplant*, 48(3), 452-458. doi:10.1038/bmt.2012.244
- 14 Klingstedt, T., Ghetti, B., Holton, J. L., Ling, H., Nilsson, K. P. R., & Goedert, M. (2019).
15 Luminescent conjugated oligothiophenes distinguish between alpha-synuclein
16 assemblies of Parkinson's disease and multiple system atrophy. *Acta Neuropathol*
17 *Commun*, 7(1), 193. doi:10.1186/s40478-019-0840-1
- 18 Laferriere, F., Maniecka, Z., Perez-Berlanga, M., Hruska-Plochan, M., Gilhespy, L., Hock, E.
19 M., . . . Polymenidou, M. (2019). TDP-43 extracted from frontotemporal lobar
20 degeneration subject brains displays distinct aggregate assemblies and neurotoxic
21 effects reflecting disease progression rates. *Nat Neurosci*, 22(1), 65-77.
22 doi:10.1038/s41593-018-0294-y
- 23 Lau, A., So, R. W. L., Lau, H. H. C., Sang, J. C., Ruiz-Riquelme, A., Fleck, S. C., . . . Watts, J.
24 C. (2019). alpha-Synuclein strains target distinct brain regions and cell types. *Nat*
25 *Neurosci*. doi:10.1038/s41593-019-0541-x
- 26 Li, B., Ge, P., Murray, K. A., Sheth, P., Zhang, M., Nair, G., . . . Jiang, L. (2018). Cryo-EM of
27 full-length alpha-synuclein reveals fibril polymorphs with a common structural
28 kernel. *Nat Commun*, 9(1), 3609. doi:10.1038/s41467-018-05971-2
- 29 Luk, K. C., Kehm, V., Carroll, J., Zhang, B., O'Brien, P., Trojanowski, J. Q., & Lee, V. M.
30 (2012). Pathological alpha-synuclein transmission initiates Parkinson-like
31 neurodegeneration in nontransgenic mice. *Science*, 338(6109), 949-953.
32 doi:10.1126/science.1227157
- 33 Masuda-Suzukake, M., Nonaka, T., Hosokawa, M., Oikawa, T., Arai, T., Akiyama, H., . . .
34 Hasegawa, M. (2013). Prion-like spreading of pathological alpha-synuclein in brain.
35 *Brain*, 136(Pt 4), 1128-1138. doi:10.1093/brain/awt037
- 36 Narasimhan, S., Guo, J. L., Changolkar, L., Stieber, A., McBride, J. D., Silva, L. V., . . . Lee, V.
37 M. Y. (2017). Pathological Tau Strains from Human Brains Recapitulate the
38 Diversity of Tauopathies in Nontransgenic Mouse Brain. *J Neurosci*, 37(47),
39 11406-11423. doi:10.1523/JNEUROSCI.1230-17.2017
- 40 Nonaka, T., Masuda-Suzukake, M., Arai, T., Hasegawa, Y., Akatsu, H., Obi, T., . . . Hasegawa,
41 M. (2013). Prion-like properties of pathological TDP-43 aggregates from diseased
42 brains. *Cell Rep*, 4(1), 124-134. doi:10.1016/j.celrep.2013.06.007

- 1 Nonaka, T., Watanabe, S. T., Iwatsubo, T., & Hasegawa, M. (2010). Seeded aggregation and
2 toxicity of {alpha}-synuclein and tau: cellular models of neurodegenerative diseases.
3 *J Biol Chem*, *285*(45), 34885-34898. doi:10.1074/jbc.M110.148460
- 4 Ohhashi, Y., Ito, K., Toyama, B. H., Weissman, J. S., & Tanaka, M. (2010). Differences in
5 prion strain conformations result from non-native interactions in a nucleus. *Nat*
6 *Chem Biol*, *6*(3), 225-230. doi:10.1038/nchembio.306
- 7 Peelaerts, W., & Baekelandt, V. (2016). α -Synuclein strains and the variable pathologies of
8 synucleinopathies. *J Neurochem*, *139 Suppl 1*, 256-274. doi:10.1111/jnc.13595
- 9 Peelaerts, W., Bousset, L., Van der Perren, A., Moskalyuk, A., Pulizzi, R., Giugliano, M., . . .
10 Baekelandt, V. (2015). α -Synuclein strains cause distinct synucleinopathies
11 after local and systemic administration. *Nature*, *522*(7556), 340-344.
12 doi:10.1038/nature14547
- 13 Peng, C., Gathagan, R. J., Covell, D. J., Medellin, C., Stieber, A., Robinson, J. L., . . . Lee, V.
14 M. (2018). Cellular milieu imparts distinct pathological α -synuclein strains in
15 α -synucleinopathies. *Nature*, *557*(7706), 558-563.
16 doi:10.1038/s41586-018-0104-4
- 17 Porta, S., Xu, Y., Restrepo, C. R., Kwong, L. K., Zhang, B., Brown, H. J., . . . Lee, V. M. (2018).
18 Patient-derived frontotemporal lobar degeneration brain extracts induce formation
19 and spreading of TDP-43 pathology in vivo. *Nat Commun*, *9*(1), 4220.
20 doi:10.1038/s41467-018-06548-9
- 21 Prusiner, S. B., Woerman, A. L., Mordes, D. A., Watts, J. C., Rampersaud, R., Berry, D. B., . . .
22 Giles, K. (2015). Evidence for α -synuclein prions causing multiple system
23 atrophy in humans with parkinsonism. *Proc Natl Acad Sci U S A*, *112*(38),
24 E5308-5317. doi:10.1073/pnas.1514475112
- 25 Ross, C. A., & Poirier, M. A. (2004). Protein aggregation and neurodegenerative disease. *Nat*
26 *Med*, *10 Suppl*, S10-17. doi:10.1038/nm1066
- 27 Saeki, Y., Isono, E., & Toh, E. A. (2005). Preparation of ubiquitinated substrates by the PY
28 motif-insertion method for monitoring 26S proteasome activity. *Methods Enzymol*,
29 *399*, 215-227. doi:10.1016/S0076-6879(05)99014-9
- 30 Saito, T., Mihira, N., Matsuba, Y., Sasaguri, H., Hashimoto, S., Narasimhan, S., . . . Saito, T.
31 C. (2019). Humanization of the entire murine Mapt gene provides a murine model of
32 pathological human tau propagation. *J Biol Chem*, *294*(34), 12754-12765.
33 doi:10.1074/jbc.RA119.009487
- 34 Shah Nawaz, M., Mukherjee, A., Pritzkow, S., Mendez, N., Rabadia, P., Liu, X., . . . Soto, C.
35 (2020). Discriminating α -synuclein strains in Parkinson's disease and multiple
36 system atrophy. *Nature*. doi:10.1038/s41586-020-1984-7
- 37 Spillantini, M. G., Schmidt, M. L., Lee, V. M., Trojanowski, J. Q., Jakes, R., & Goedert, M.
38 (1997). α -Synuclein in Lewy bodies. *Nature*, *388*(6645), 839-840.
39 doi:10.1038/42166

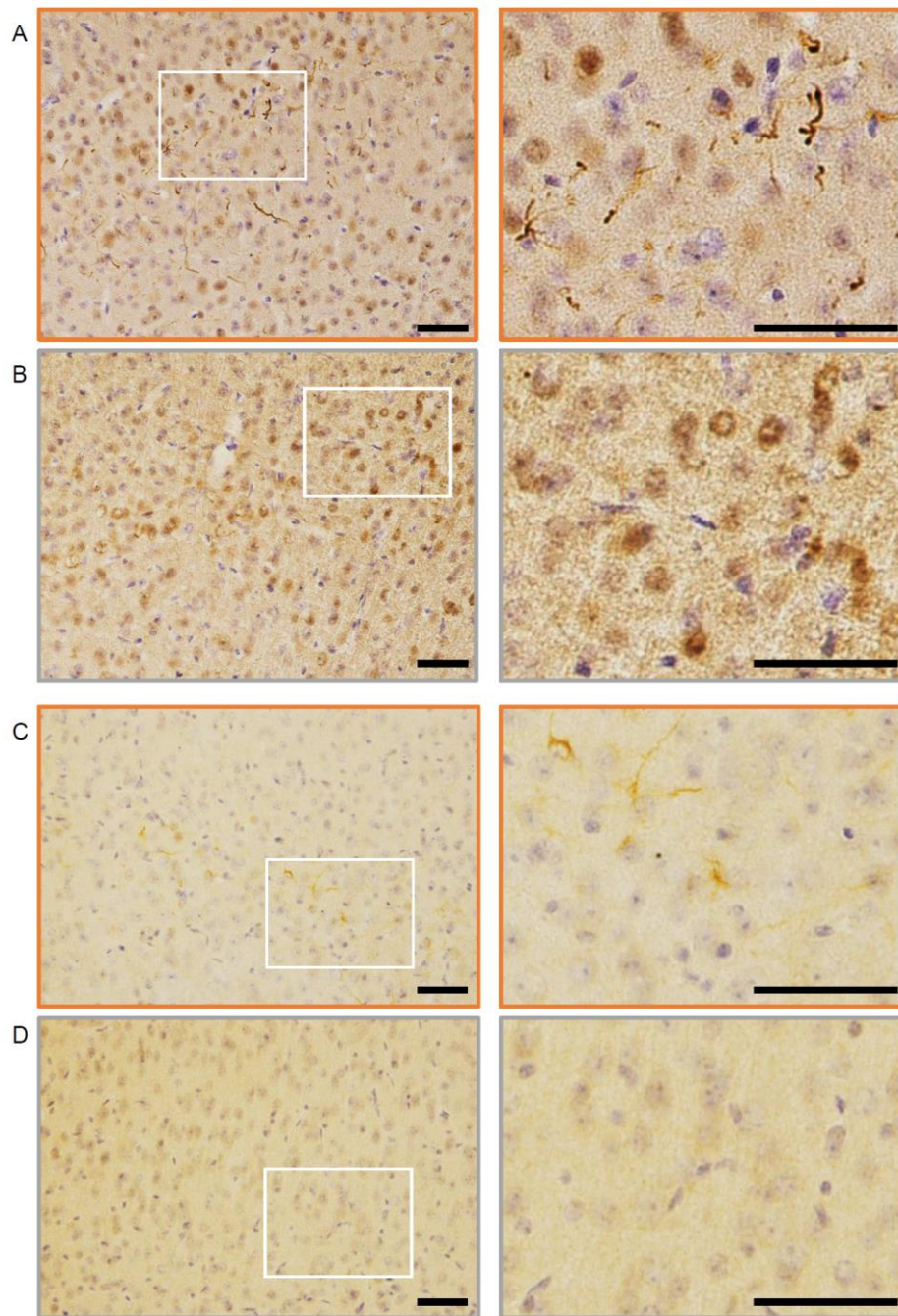
- 1 Suzuki, G., Shimazu, N., & Tanaka, M. (2012). A yeast prion, Mod5, promotes acquired drug
2 resistance and cell survival under environmental stress. *Science*, *336*(6079), 355-359.
3 doi:10.1126/science.1219491
- 4 Tarutani, A., Arai, T., Murayama, S., Hisanaga, S. I., & Hasegawa, M. (2018). Potent
5 prion-like behaviors of pathogenic alpha-synuclein and evaluation of inactivation
6 methods. *Acta Neuropathol Commun*, *6*(1), 29. doi:10.1186/s40478-018-0532-2
- 7 Terada, M., Suzuki, G., Nonaka, T., Kametani, F., Tamaoka, A., & Hasegawa, M. (2018). The
8 effect of truncation on prion-like properties of alpha-synuclein. *J Biol Chem*, *293*(36),
9 13910-13920. doi:10.1074/jbc.RA118.001862
- 10 Thibautaud, T. A., Anderson, R. T., & Smith, D. M. (2018). A common mechanism of
11 proteasome impairment by neurodegenerative disease-associated oligomers. *Nat*
12 *Commun*, *9*(1), 1097. doi:10.1038/s41467-018-03509-0
- 13 Tsuji, H., Arai, T., Kametani, F., Nonaka, T., Yamashita, M., Suzukake, M., . . . Tamaoka, A.
14 (2012). Molecular analysis and biochemical classification of TDP-43 proteinopathy.
15 *Brain*, *135*(Pt 11), 3380-3391. doi:10.1093/brain/aws230
- 16 Wakabayashi, K., Yoshimoto, M., Tsuji, S., & Takahashi, H. (1998). Alpha-synuclein
17 immunoreactivity in glial cytoplasmic inclusions in multiple system atrophy.
18 *Neurosci Lett*, *249*(2-3), 180-182. doi:10.1016/s0304-3940(98)00407-8
- 19 Watts, J. C., Giles, K., Oehler, A., Middleton, L., Dexter, D. T., Gentleman, S. M., . . .
20 Prusiner, S. B. (2013). Transmission of multiple system atrophy prions to transgenic
21 mice. *Proc Natl Acad Sci U S A*, *110*(48), 19555-19560. doi:10.1073/pnas.1318268110
- 22 Woerman, A. L., Oehler, A., Kazmi, S. A., Lee, J., Halliday, G. M., Middleton, L. T., . . .
23 Prusiner, S. B. (2019). Multiple system atrophy prions retain strain specificity after
24 serial propagation in two different Tg(SNCA*A53T) mouse lines. *Acta Neuropathol*,
25 *137*(3), 437-454. doi:10.1007/s00401-019-01959-4
- 26 Woerman, A. L., Stohr, J., Aoyagi, A., Rampersaud, R., Krejciova, Z., Watts, J. C., . . .
27 Prusiner, S. B. (2015). Propagation of prions causing synucleinopathies in cultured
28 cells. *Proc Natl Acad Sci U S A*, *112*(35), E4949-4958. doi:10.1073/pnas.1513426112
- 29 Wong, Y. C., & Krainc, D. (2017). alpha-synuclein toxicity in neurodegeneration: mechanism
30 and therapeutic strategies. *Nat Med*, *23*(2), 1-13. doi:10.1038/nm.4269
- 31 Zondler, L., Kostka, M., Garidel, P., Heinzlmann, U., Hengerer, B., Mayer, B., . . . Danzer, K.
32 M. (2017). Proteasome impairment by alpha-synuclein. *PLoS One*, *12*(9), e0184040.
33 doi:10.1371/journal.pone.0184040

34

35



- 1 **Figure 1.** Preparation and characterization of two α -synuclein strains.
- 2 (A) Schematic representation of two α -synuclein (α S) strains (left) and the resulted two
3 α -synuclein assemblies (right). (B) Turbidity of these assemblies. Analysis was performed using
4 student t test. (mean \pm S.E.M; n=3) Formation of aggregates rather than soluble oligomer is
5 shown in Figure 1-figure supplement 1. (C) Transfer electron microscopy (TEM) images of
6 these assemblies. Scale bar, 200nm. (D) Thioflavin T fluorescence of these assemblies and α S
7 monomer. Analysis was performed using one-way ANOVA and Tukey post hoc test.
8 (mean \pm S.E.M; n=3) (E) Congo red bindings of these strains and α S monomer. (mean \pm S.E.M;
9 n=3) (F) In vitro seeding activity of these strains. α -synuclein monomers were incubated with
10 α -synuclein fibril (-) (orange) or α -synuclein fibril (+) (gray). Kinetics of Thioflavin T
11 fluorescence were shown. Analysis was performed using one-way ANOVA and Tukey post hoc
12 test. **P<0.01, ***P<0.001, ****P<0.0001.
- 13 **Source Data 1.** Quantification for graph in Figure 1B, D and E.
- 14 **Source Data 2.** Three independent data in Figure 1F.

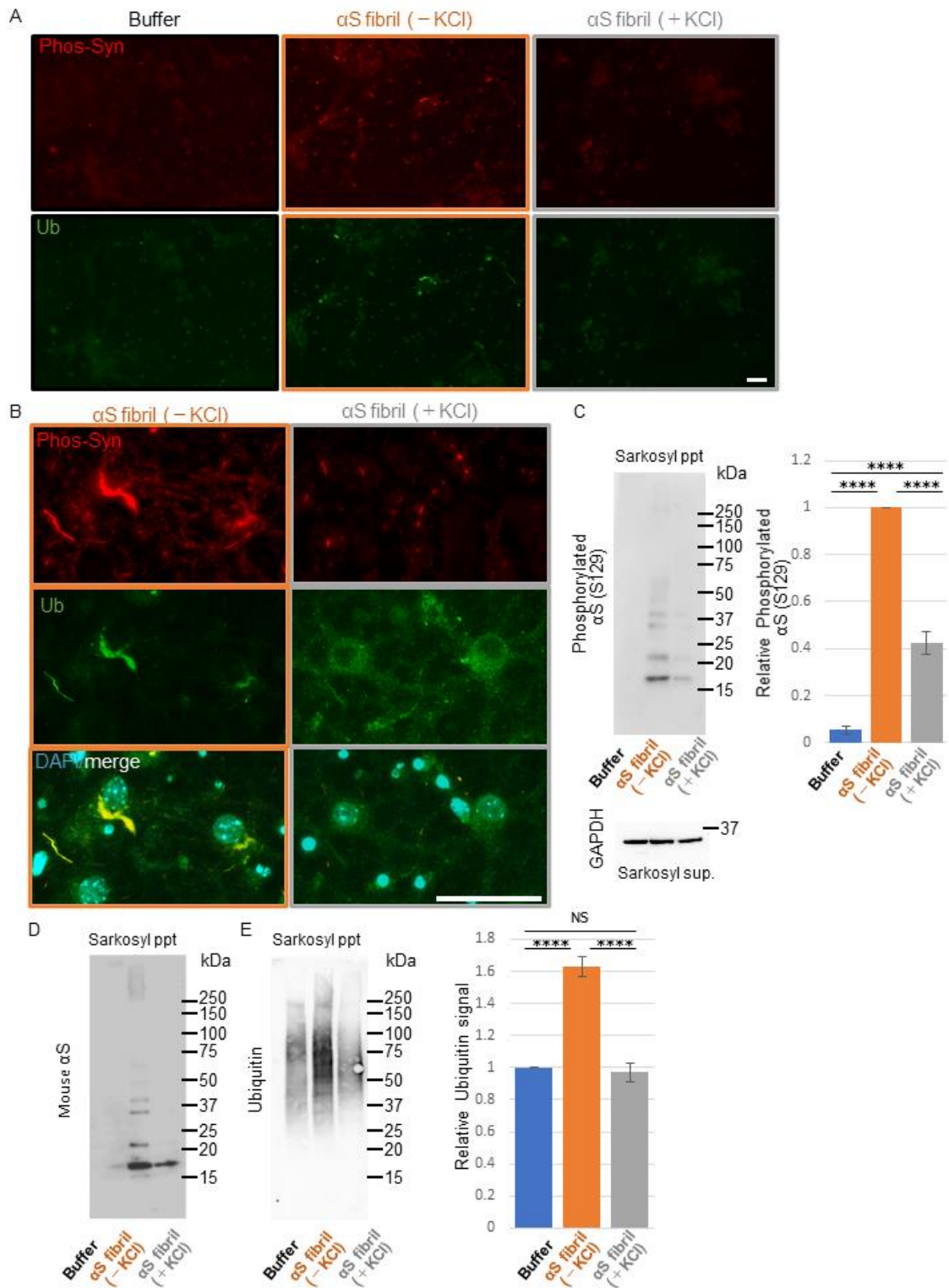


1
2

3 **Figure 2.** Comparison of pathologies in WT mouse brains by inoculation of two a-synuclein
4 strains.

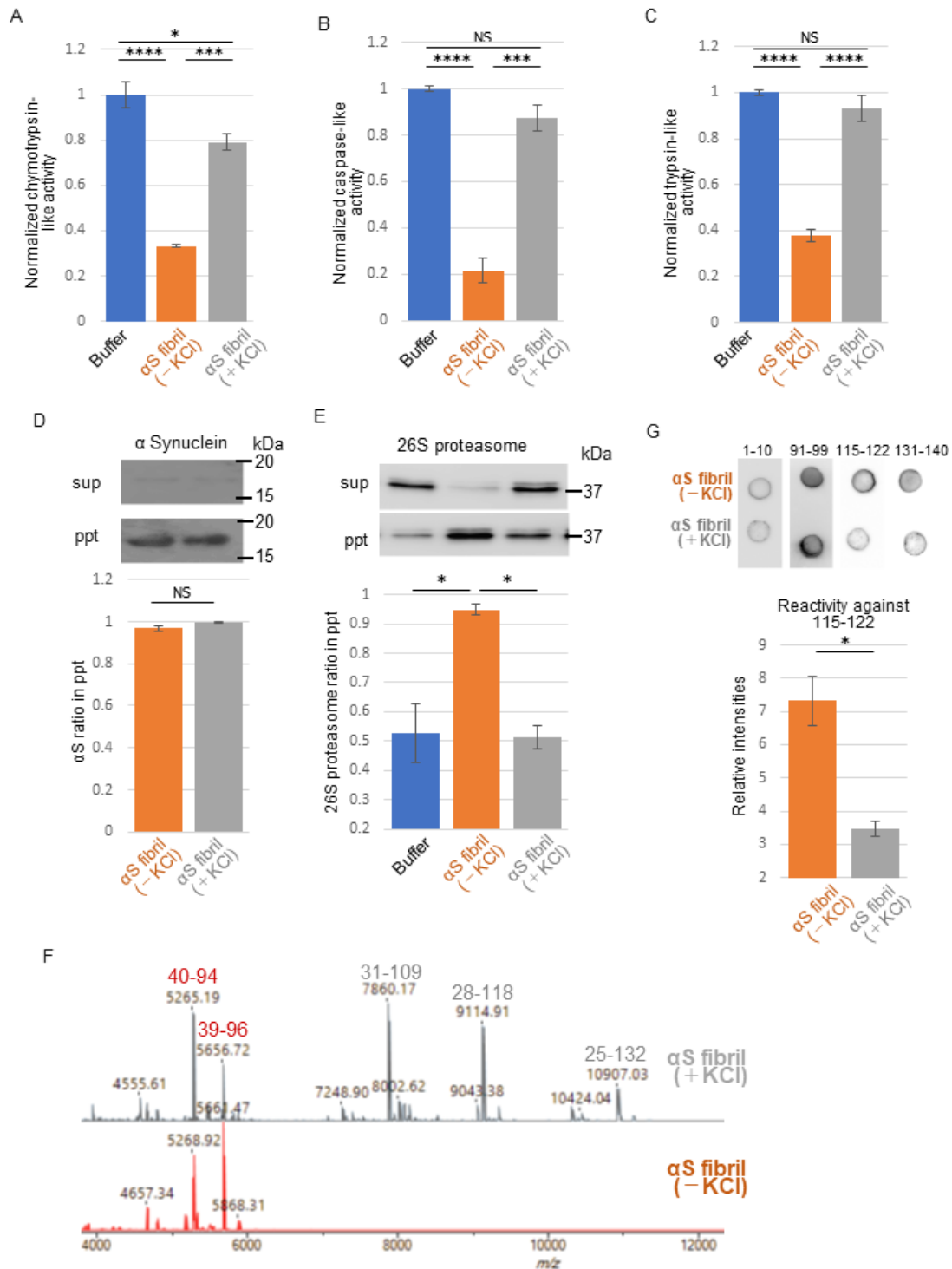
5 (A and B) Distribution of phosphorylated a-synuclein pathology in mouse brain. a-synuclein
6 fibrils (-) (A) or a-synuclein fibrils (+) (B) were injected into WT mouse brain and stained with

1 phosphorylated a-synuclein antibody 1 month after injection. Representative images of cortex
2 are shown. Representative images of corpus callosum and striatum are shown in Figure 2-figure
3 supplement 1. Regions surrounded by white rectangles in left panels were magnified and shown
4 in right panels. Sections were counterstained with hematoxylin. (C and D) Distribution of
5 ubiquitin pathology in mouse brain. a-synuclein fibrils (-) (C) or a-synuclein fibrils (+) (D) were
6 injected into WT mouse brain and stained with ubiquitin antibody 1 month after injection.
7 Regions surrounded by white rectangles in left panels were magnified and shown in right
8 panels. Sections were counterstained with hematoxylin. Scale bars, 50 mm.
9



1
2

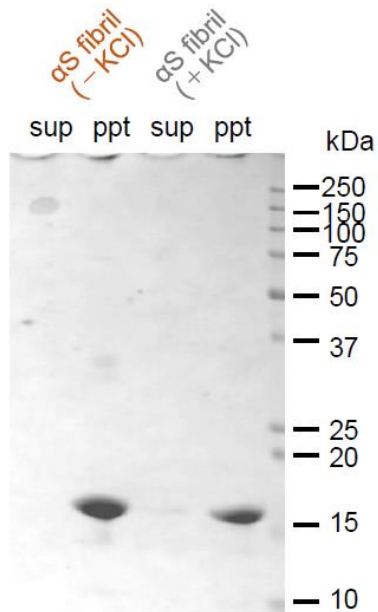
1 **Figure 3.** Seeding activities α -synuclein strains in primary neurons.
2 (A) α -synuclein strains were transduced into mouse primary neurons. 14 days after fibril
3 transduction, the accumulation of abnormal phosphorylated α -synuclein (Phos-Syn, upper) and
4 ubiquitinated aggregates (Ub, lower) are detected by immunofluorescence microscopy. Scale
5 bar, 50 μ m (B) Higher magnification images of primary neurons treated with α -synuclein
6 fibrils. Cells were stained with phosphorylated α -synuclein, ubiquitin and DAPI. Scale bar 50
7 μ m. (C) Detection of sarkosyl insoluble phosphorylated α -synuclein by western blotting (left,
8 upper) and the quantification data (mean \pm S.E.M; n=3) (right). Detection of sarkosyl soluble
9 GAPDH as a loading control (left, lower). (D) Detection of sarkosyl insoluble endogenous
10 mouse α -synuclein by western blotting. (E) Detection of sarkosyl insoluble ubiquitinated
11 proteins by western blotting (left) and the quantification data (mean \pm S.E.M; n=3) (right).
12 Analysis was performed using one-way ANOVA and Tukey post hoc test. ****P<0.0001.
13 **Source Data 1.** Quantification for graph in Figure 3C and E.
14



1
2

1 **Figure 4.** Different interaction of α -synuclein strains with 26S proteasome
2 (A-C) Effects of the α -synuclein strains on the 26S proteasome activity. 26S proteasome was
3 purified from budding yeast as shown in Figure 4-figure supplement 1. 26S proteasome
4 activities in the presence of α -synuclein strains were measured. Chymotrypsin like activity was
5 measured by LLVY-MCA hydrolysis(A). Caspase like activity was measured by LLE-MCA
6 hydrolysis (B). Trypsin like activity was measured by LRR-MCA hydrolysis (mean \pm S.E.M;
7 n=3). (D and E) Co-precipitation of 26S proteasome with the α -synuclein strains. 26S
8 proteasome was mixed with the α -synuclein strains and centrifuged. Resulted supernatant (sup)
9 and pellet (ppt) fractions were analyzed by western blotting against α -synuclein (D, upper) and
10 Rpn11-HA (E, upper). Quantification of the α -synuclein (D, lower) and Rpn11-HA (E, lower) in
11 ppt fractions were shown. (mean \pm S.E.M; n=3) (F) The core regions of the α -synuclein strains.
12 These α -synuclein strains were mildly digested by proteinase K and centrifuged. The resulted
13 pellet fractions were denatured by guanidine and analyzed by MALDI-TOF-MS. Peptide peaks
14 identified by mass analysis and the predicted peptide regions corresponding to each peak were
15 shown. (G) Dot blot analysis of the α -synuclein strains. These α -synuclein strains were spotted
16 on nitrocellulose membranes and detected by various antibodies against α -synuclein (upper).
17 Reactivity against the antibody raised against 115-122 region of α -synuclein was quantified
18 (mean \pm S.E.M; n=3) (lower). Analysis was performed using one-way ANOVA and Tukey post
19 hoc test. *P<0.05, ***P<0.001, ****P<0.0001 (A, B, C and F). Analysis was performed using
20 student t test. *P<0.05 (D and G). Seeding activities of C-terminal truncated α -synuclein fibrils
21 in primary neurons are shown in Fugure 4-figure supplement 2. Schematic model of α -synuclein
22 strain formation and strain dependent interaction and inhibition with 26S proteasome is shown
23 in Figure 4-figure supplement 3.
24 **Source Data 1.** Quantification for graph in Figure 4A, B and C.
25 **Source Data 2.** Quantification for graph in Figure 4D, E and G.

1 Figure Supplement



2

3

4 Figure 1-figure supplement 1

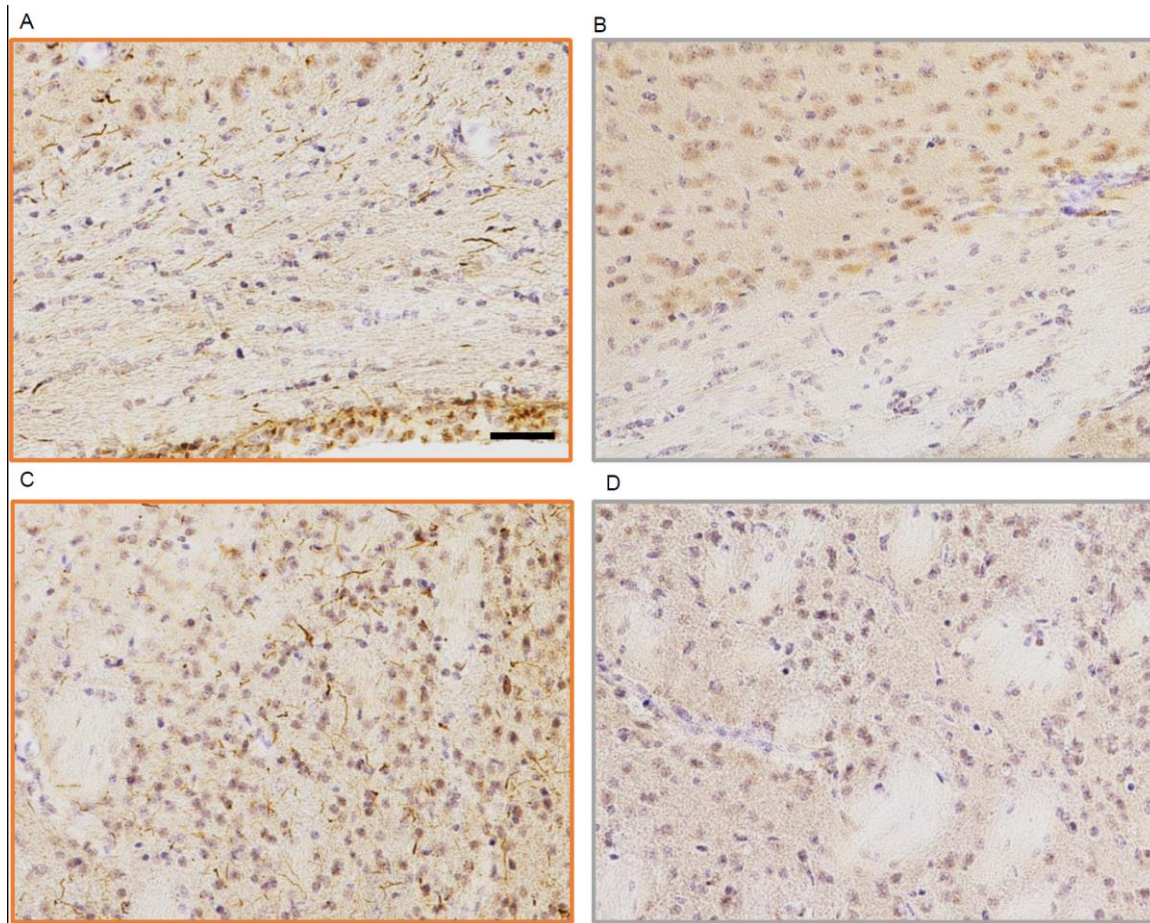
5 Formation of α -synuclein aggregates.

6 α -synuclein monomers are incubated for 7days and then centrifuged at 10,000 x g for 10 min to

7 separate soluble oligomers and insoluble aggregates. CBB staining of soluble fractions (sup)

8 and insoluble fractions (ppt) are shown. Soluble oligomers are hardly detected in both

9 α -synuclein strains.



1

2 **Figure2-figure supplement 1**

3 Comparison of pathologies in WT mouse brains by inoculation of two α -synuclein strains.

4 Distribution of phosphorylated α -synuclein pathology in mouse brain. α -synuclein fibrils (-) (A

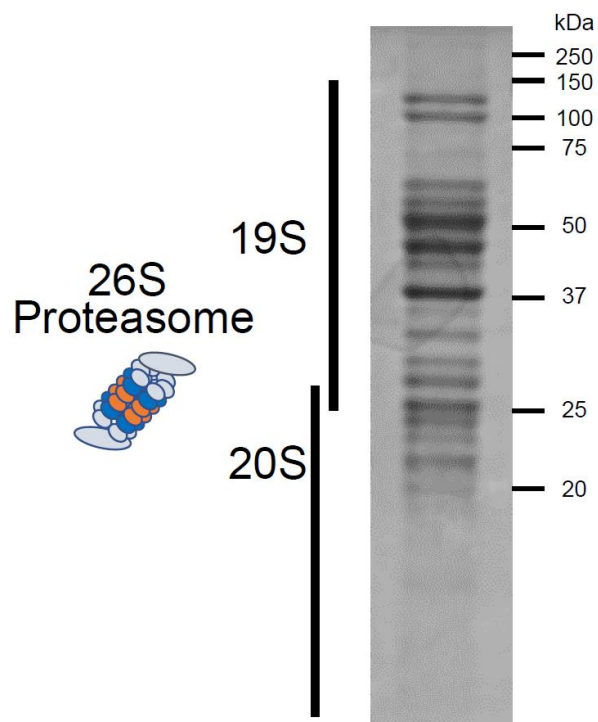
5 and C) or α -synuclein fibrils (+) (B and D) were injected into WT mouse brain and stained with

6 phosphorylated α -synuclein antibodies 1 month after injection. Representative images of corpus

7 callosum (A and B) and striatum (C and D) are shown. Sections were counterstained with

8 hematoxylin. Scale bar, 50 μ m.

9



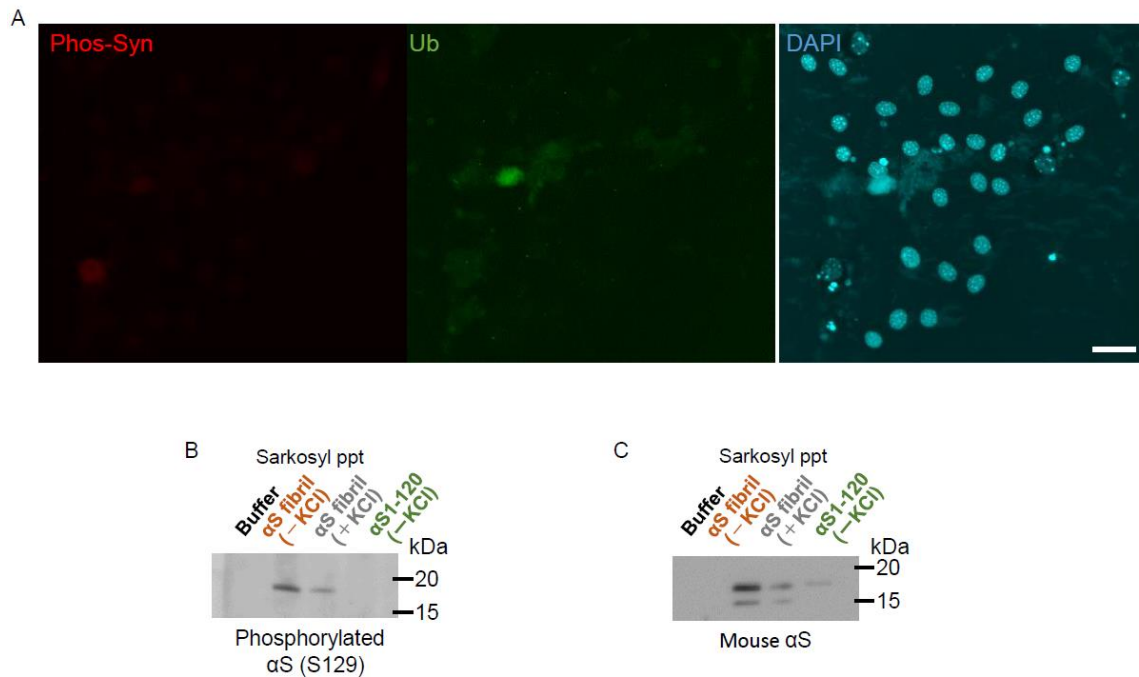
1

2 **Figure 4-figure supplement 1**

3 Purification of 26S proteasome.

4 CBB staining of 26S proteasome complex used in this study.

5



1 **Figure 4-figure supplement 2**

2 Seeding activities of C-terminal truncated α -synuclein fibrils in primary neurons.

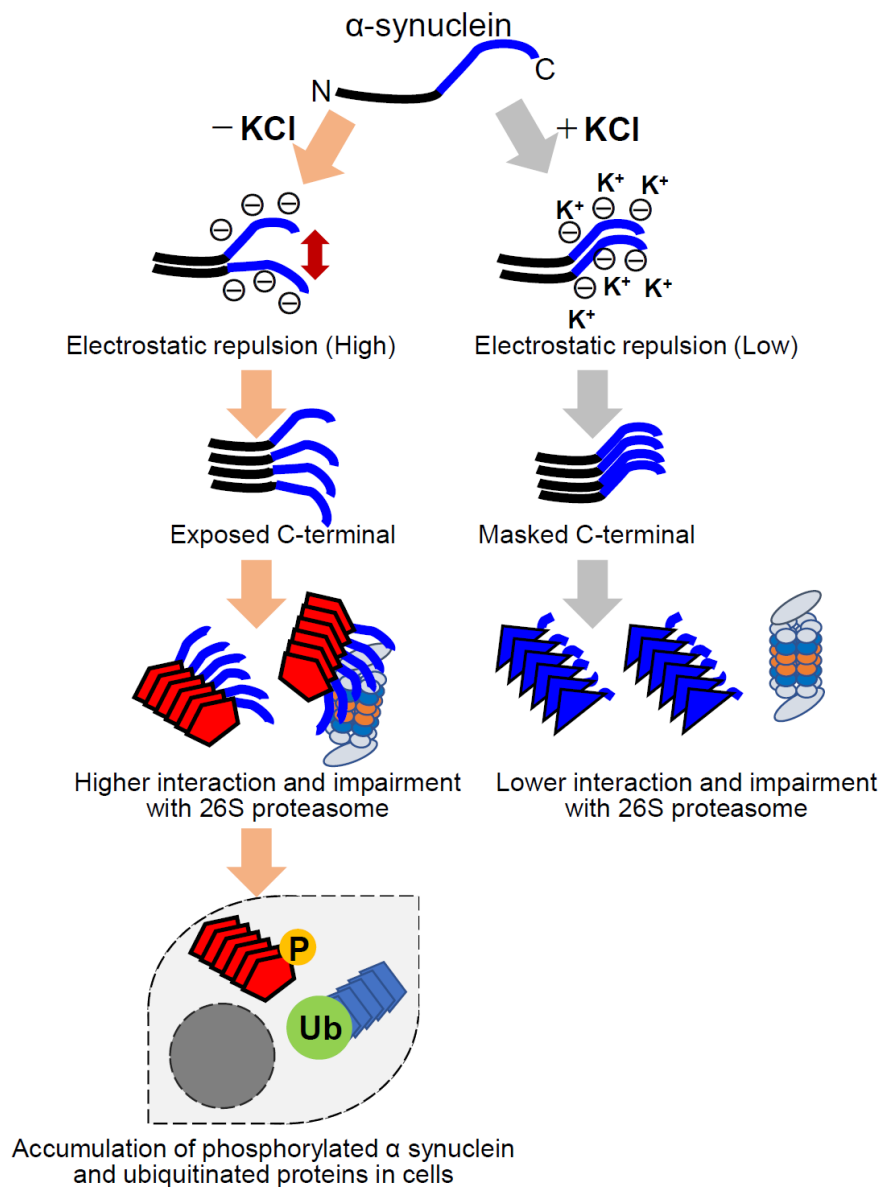
3 (A) C-terminal truncated α -synuclein fibrils were transduced into mouse primary neurons. 14

4 days after fibril transduction, the accumulation of abnormal phosphorylated α -synuclein

5 (Phos-Syn, left) and ubiquitinated aggregates (Ub, center) are detected by immunofluorescence

6 microscopy. Scale bar, 50 μ m (B) Detection of sarkosyl insoluble phosphorylated α -synuclein

7 by western blotting. (C) Detection of sarkosyl insoluble mouse α -synuclein by western blotting.



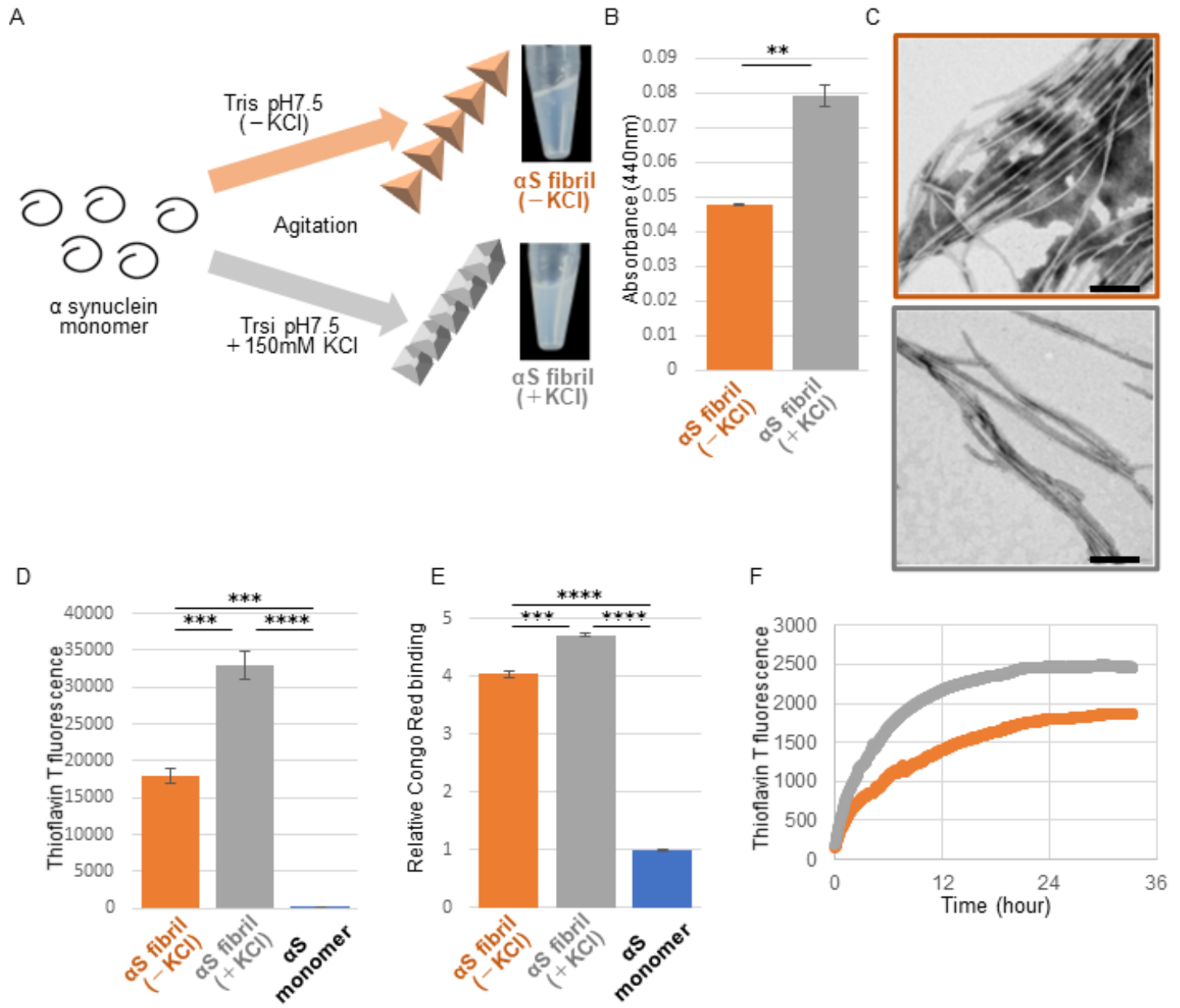
1

2 **Figure 4-figure supplement 3**

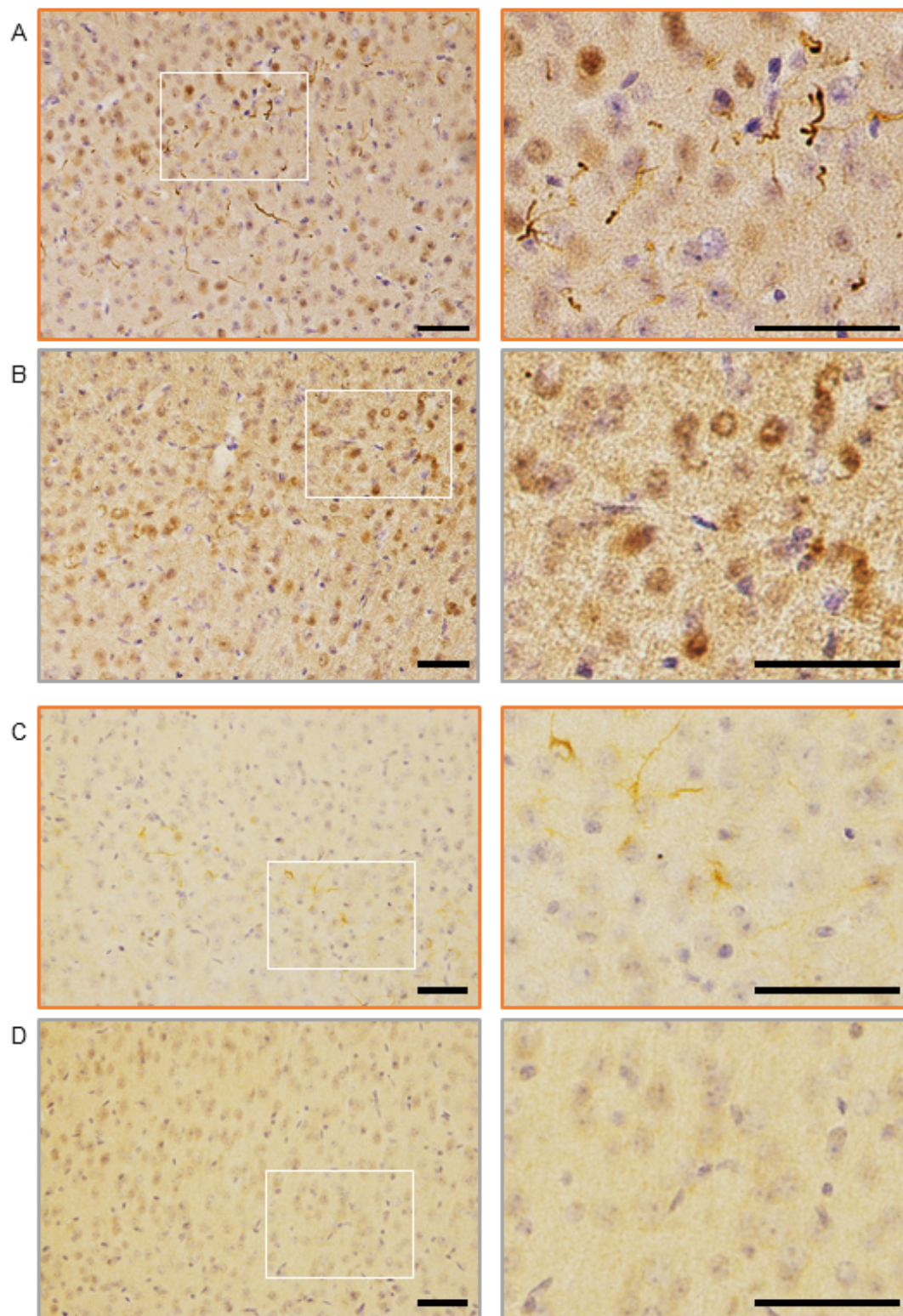
3 Schematic representation of α -synuclein strain formation and strain dependent interaction with
4 26S proteasome.

5 In the absence of salt, α -synuclein monomers have exposed C-terminal region with high electric
6 repulsion. These form the α -synuclein strain with exposed C-terminal region and this type of the
7 α -synuclein strain can interact with 26S proteasomes and inhibit their activities resulting the
8 accumulation of phosphorylated α -synuclein aggregates and ubiquitinated proteins (left). In the

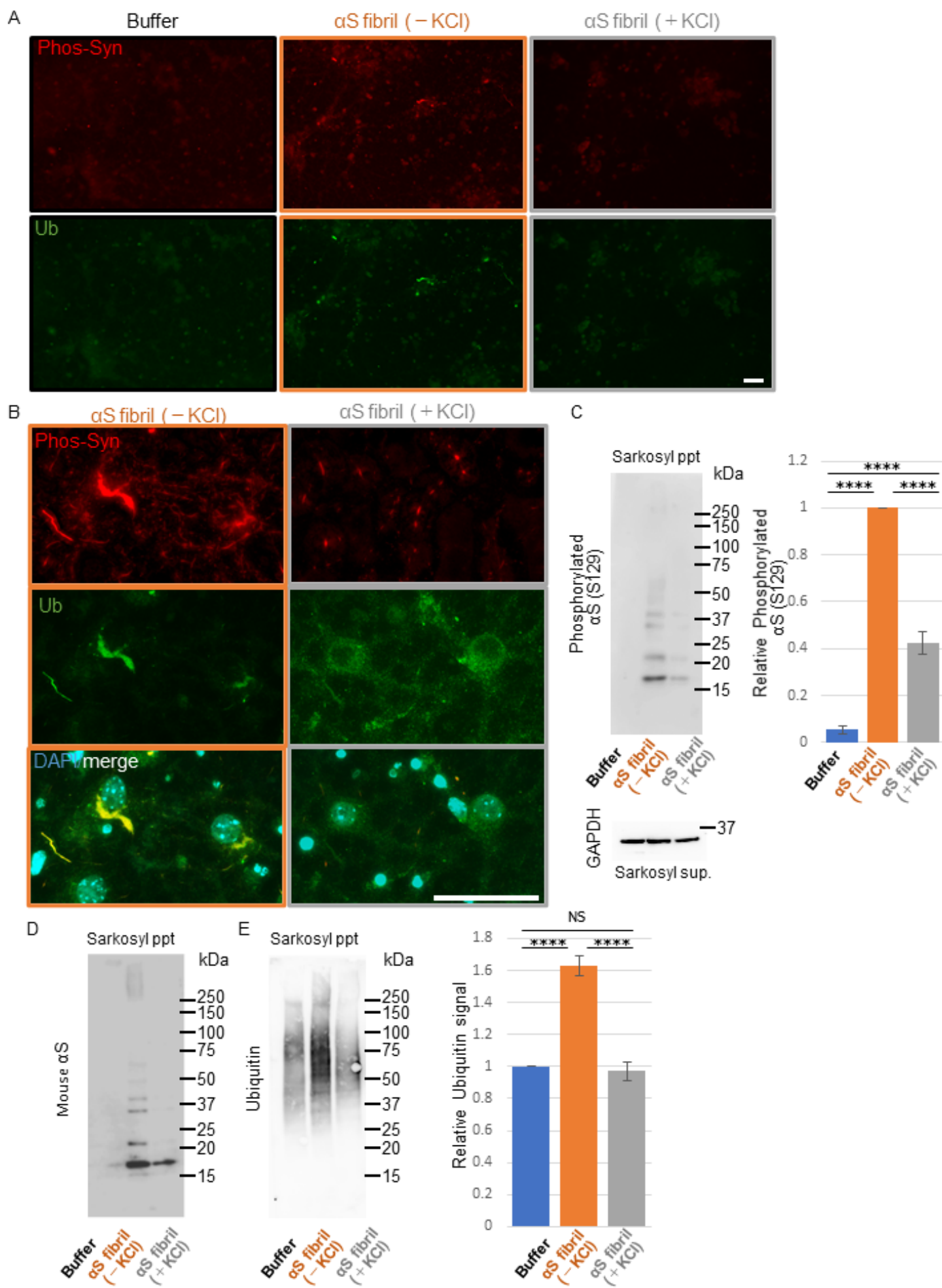
- 1 presence of salt, α -synuclein monomers have packed C-terminal region with low electric
- 2 repulsion. These form the α -synuclein strain with masked C-terminal region and this type of the
- 3 α -synuclein strain can not interact with 26S proteasomes.
- 4
- 5



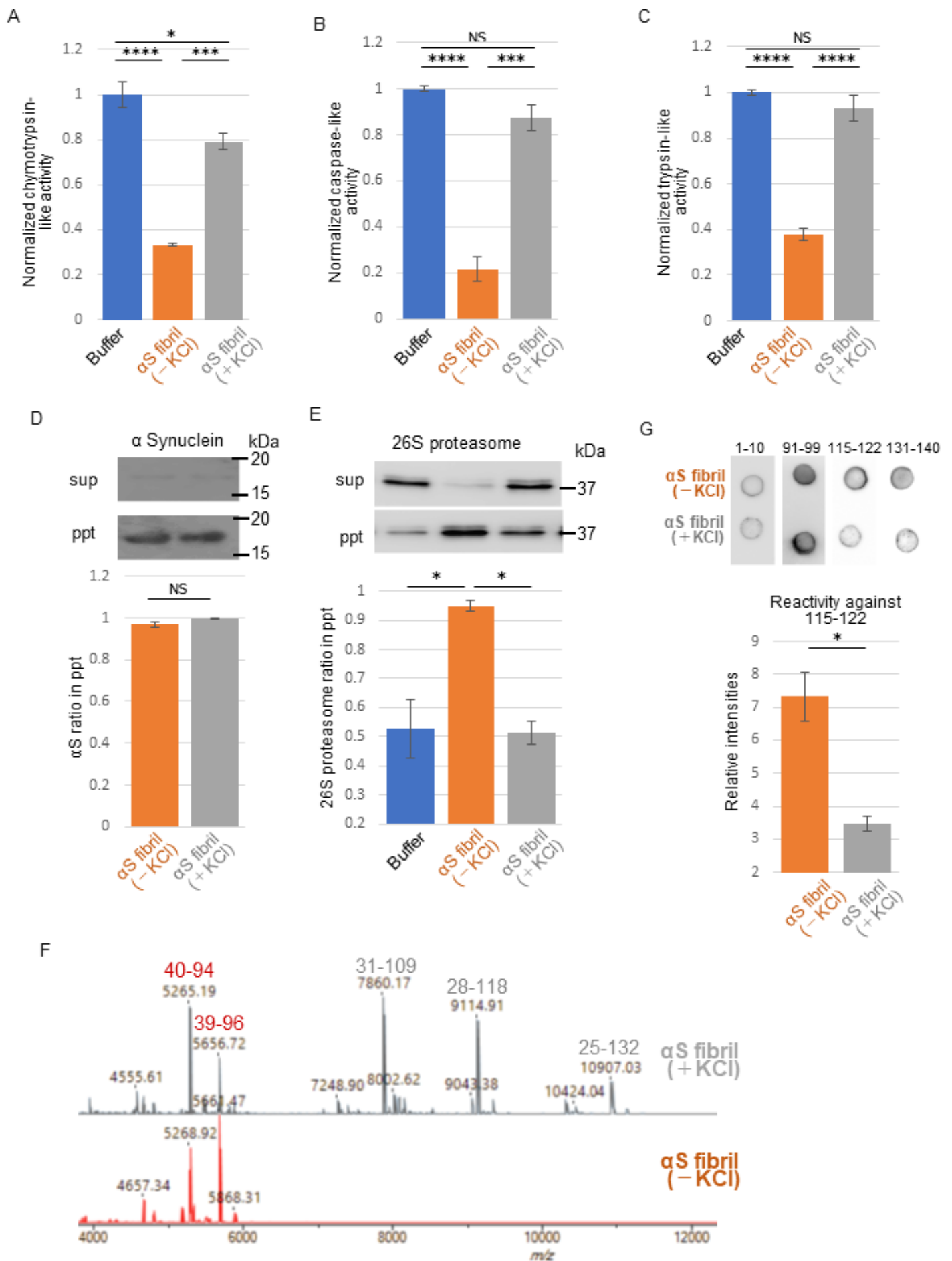
Suzuki et al., Figure 1.



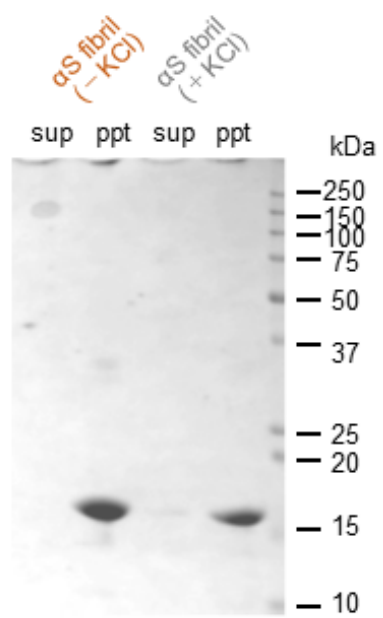
Suzuki et al., Figure 2.



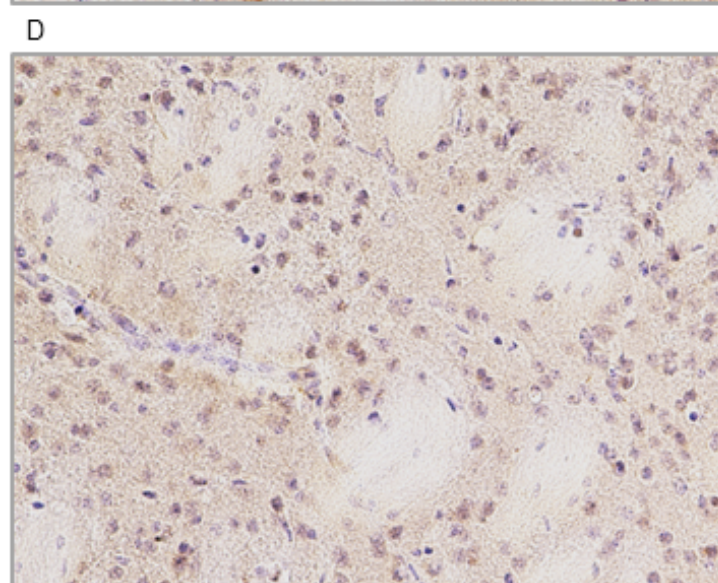
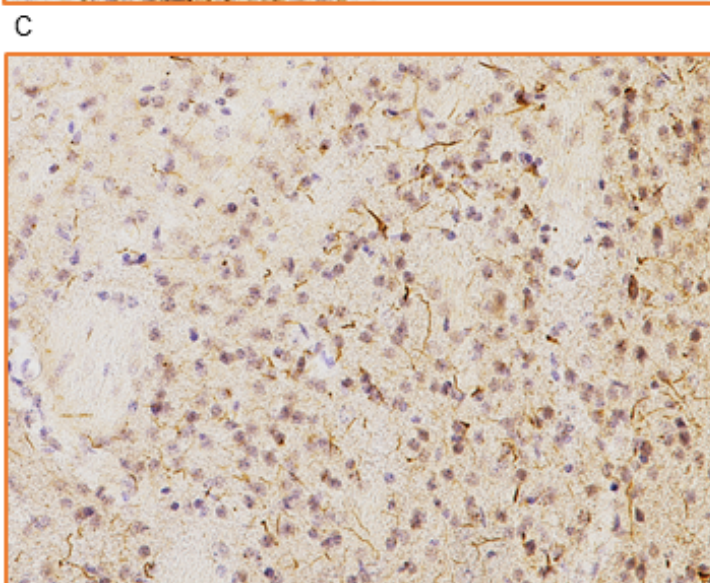
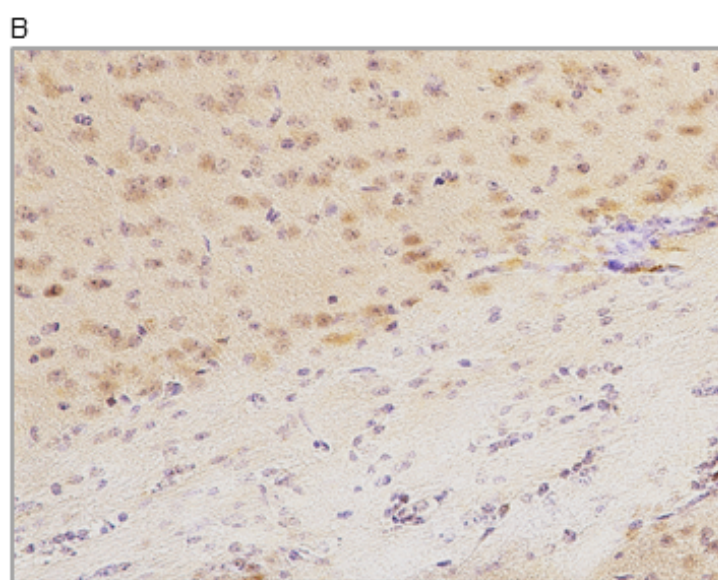
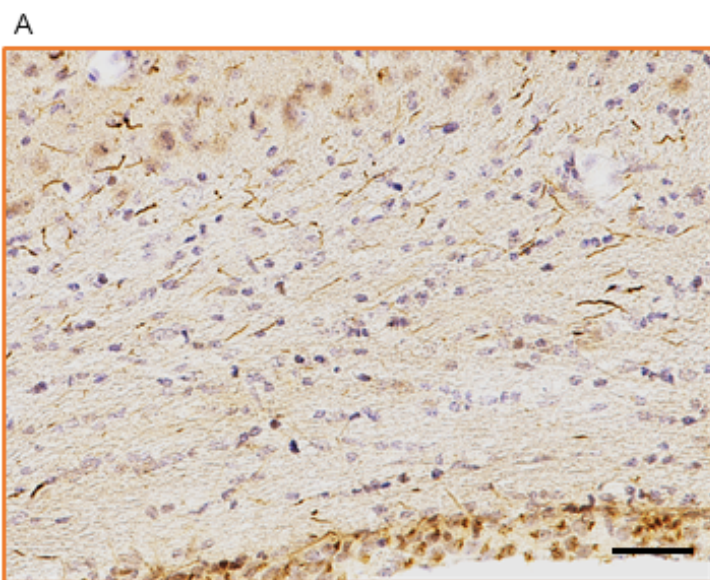
Suzuki et al., Figure 3.



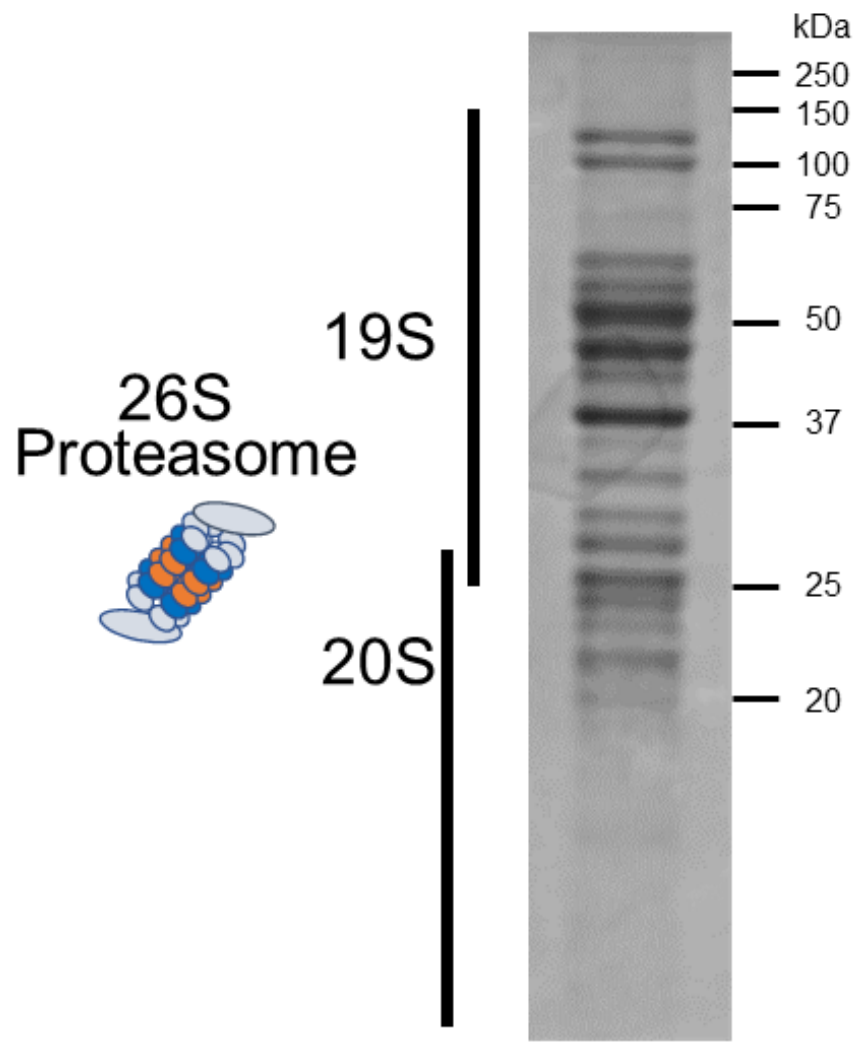
Suzuki et al., Figure 4.



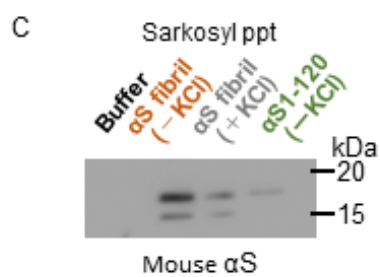
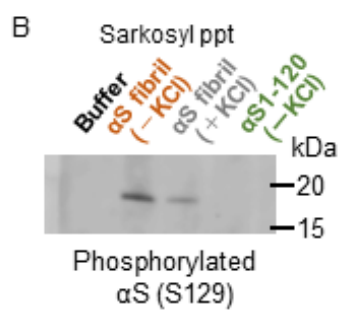
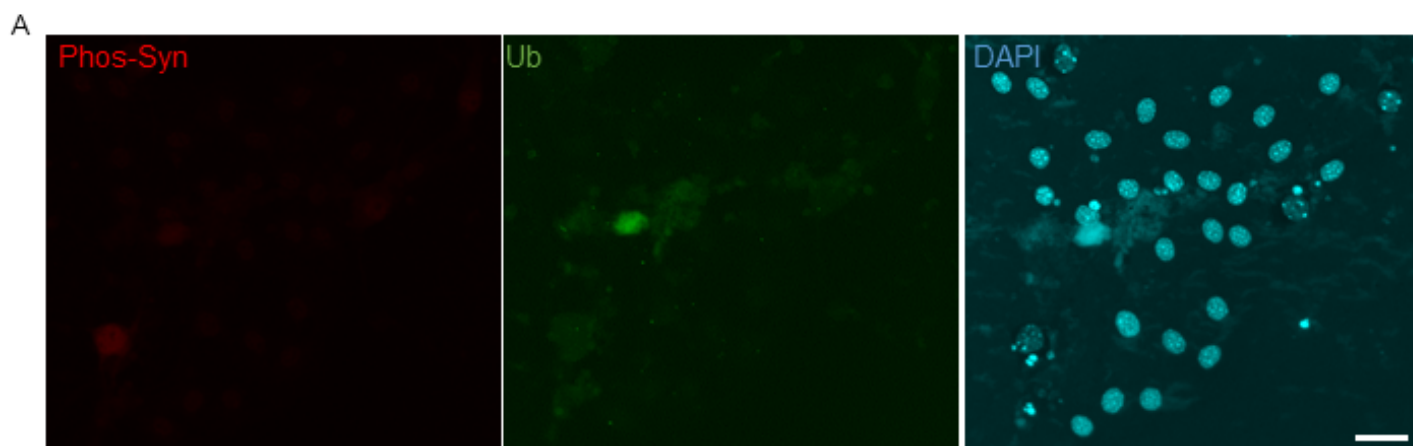
Suzuki et al., Figure 1-figure supplement 1



Suzuki et al., Figure 2-figure supplement 1



Suzuki et al., Figure 4-figure supplement 1



Suzuki et al., Figure 4-figure supplement 2

